

LAMINAR BOUNDARY LAYER OVER A CONE
AT AN ANGLE OF ATTACK IN CONICAL FLOW

BY
PRADEEP KUMAR

AE
1972
M
RAO
LAM

TH
AE/1972/M
K961



DEPARTMENT OF AERONAUTICAL ENGINEERING
INDIAN INSTITUTE OF TECHNOLOGY KANPUR
NOVEMBER 1972

✓ **LAMINAR BOUNDARY LAYER OVER A CONE
AT AN ANGLE OF ATTACK IN CONICAL FLOW**

A Thesis Submitted
In Partial Fulfilment of the Requirements
for the Degree of
MASTER OF TECHNOLOGY

2082
BY
PRADEEP KUMAR

to the

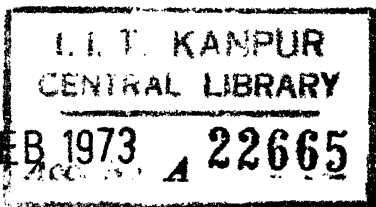
DEPARTMENT OF AERONAUTICAL ENGINEERING
INDIAN INSTITUTE OF TECHNOLOGY KANPUR
NOVEMBER 1972

Thesis



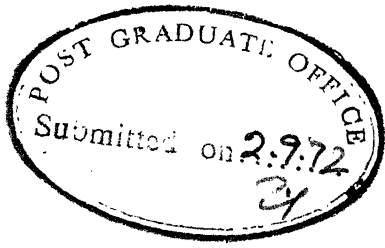
6295237

P 882



AE-1972-m-~~KLM~~-LAM

PRA



CERTIFICATE

Certified that this work on 'LAMINAR BOUNDARY LAYER OVER A CONE AT AN ANGLE OF ATTACK IN CONICAL FLOW' has been carried out under my supervision and that this has not been submitted elsewhere for a degree.

N. Nigam
+ (A.C. JAIN)
Department of Aeronautical Engineering
Indian Institute of Technology, Kanpur

POST GRADUATE OFFICE
This thesis is hereby accepted for the award of the degree of Master of Science (Aeronautical Engineering) in accordance with the regulations of the Indian Institute of Technology
Dated. 4.1.78 21

ACKNOWLEDGEMENT

The author is deeply grateful to Dr. A.C. Jain for suggesting this problem, and for the invaluable guidance, help and encouragement rendered to him during the course of development of this work. He is also grateful to his friends, who helped him at various stages of this work. He expresses his thanks to Mr. S.Kumar, who did an efficient job of presenting the matter in this form.

CONTENTS

	Page
ABSTRACT	
LIST OF SYMBOLS	
CHAPTER 1 INTRODUCTION	1
CHAPTER 2 GENERAL ANALYSIS	23
CHAPTER 3 RESULTS	55
REFERENCES	62
APPENDIX 1	66
APPENDIX 2	73
APPENDIX 3	83
FIGURES	

ABSTRACT

Locally similar solutions for boundary layer on a circular cone in assymmetric conical flow is analysed in spherical polar coordinates. A series solution in the ascending powers of angle of attack α and thickness parameter ξ , that is the ratio of local boundary layer thickness to the local radius of transverse curvature, is developed. The various terms of this series are split into universal functions, which are independent of prescribed conditions namely, semi-vertex cone angle and the free stream conditions. The leading term is the well known Blaussius Equation and the remaining equations are linear and form a recursive set of equations. These equations are integrated numerically using Runge-Kutta Method. Though only first order terms in α and ξ are considered in this analysis, it can be extended to consider higher order terms in α and ξ .

- - -

LIST OF SYMBOLS

c_o	Chapman-Rubisen constant
c_f	coefficient of friction
f	stream function related to meridinal velocity, defined by Equation (2.1.26)
\bar{f}	stream function related to meridinal velocity, defined by Equation (2.1.21)
g	stream function related to circumferential velocity, defined by Equation (2.1.21)
F	universal functions related to meridinal velocity
G	universal functions related to circumferential velocity
H	total enthalpy, non-dimensional, defined by Equation (2.1.6)
L	differential operator, defined by (2.3.20)
L_1	differential operator, defined by (2.3.28)
M	Mach Number
p	pressure
r	distance from vertex of cone
r_o	local transverse radius of cone
R	non-dimensional distance from vertex of cone
Re_L	Reynold number
Re_r	local Reynold number

T	Temperature
u	meridinal velocity
v	velocity normal to the surface of cone
w	circumferential velocity
x	perturbation in meridinal velocity due to angle of attack in inviscid flow over cone
y	perturbation in circumferential velocity due to angle of attack in inviscid flow over cone
z	perturbation in density due to angle of attack in inviscid flow over cone

SUBSCRIPTS AND SUPERSCRIPTS

o	conditions at surface of cone at zero angle of attack in inviscid flow
e	conditions at the edge of boundary layer
-	denotes dimensional variables
'	differentiation with respect to similarity variable

GREEK SYMBOLS

α	angle of attack
β	defined by Equation (2.1.15)
γ	ratio of specific heats
δ	boundary layer thickness
δ_r^*	displacement thickness-associated with u

δ_ϕ^*	displacement thickness-associated with w
η	similarity variable, defined by Equation (2.1.21)
θ_c	semi-vertex cone angle
θ	angle between radius vector and cone axis
ω	defined by Equation (2.1.6)
λ	perturbation in pressure due to angle of attack in inviscid flow over a cone
μ	coefficient of viscosity
ξ	thickness parameter, defined by (2.1.20)
ρ	density
τ	shear stress
ϕ	azimuthal angle
χ, ψ	stream functions, defined by Equation (2.1.13)

CHAPTER 1

INTRODUCTION

Motivation and Scope of the Problem

When a slender cone is placed in supersonic stream, the inviscid flow over the cone is conical in nature, that is flow properties do not change along a ray from the vertex of the cone. This holds for the case of a cone at an angle of attack also. If the fluid is viscous there is a boundary layer formation on the surface of the cone. The conical inviscid flow affects the detailed structure of the flow in the boundary layer and provides the necessary boundary conditions at the edge of the boundary layer. At an angle of attack, pressure on the wind-ward side is higher than the pressure on the leeward side, and thus there exists a circumferential pressure gradient. Since near the surface of the cone, the inertia of the fluid is less than that on the edge, fluid near the surface tend to move in the direction of pressure gradient more closely than the fluid near the edge. Hence low energy fluid near the surface is drained from windward side to leeward side. Thus thickness of the boundary layer is more on leeward side than on the windward side. In the forward region of the cone, the thickness of the boundary layer is comparable with the transverse curvature of the cone. This is more so on t

leeward side of the cone. Thus considering the locally similar boundary layer, it is possible to predict the results more accurately near the vertex of the cone and one can go far down the leeward side.

We know that boundary layer grows thicker as the Mach number in the external stream increases. At hypersonic speeds, boundary layer remains no longer thin on most part of the cone in comparison to the transverse ^{radius of} curvature of the cone. Hence, thickness effects should be considered in any analytical development of the boundary layer flows, at high Mach numbers.

From the above physical consideration, it has been found necessary to consider the locally similar boundary layer and estimate more accurately the detailed structure and the overall characteristics of the boundary layer flow over the cone at angle of attack.

From mathematical point of view, we hope to gain an advantage over the existing approaches to solve this problem. Most of the boundary layer analysis is carried out in the cylindrical polar coordinate system, while for the cone

problem, spherical polar coordinate system seems to be more natural. Because, all the inviscid flow analysis are in spherical polar coordinate system and this coordinate system eliminates the need of using Mangler's transformation, to convert the equations of motion to almost Cartesian form. In the present investigation, boundary layer flow is analysed in spherical polar coordinates. A similarity transformation is found for this coordinate system and a series solution in the ascending powers of the angle of attack, α , and thickness parameter ϵ .

$$\xi = \sqrt{\frac{C_0}{Re_0}} \frac{\cot \theta_c}{r} \sqrt{\frac{L}{r}}$$

where C_0 - Chapman Rubisen const

$$Re_0 - \text{Reynold No.} = \frac{P_0 U_0 L}{\mu_0}$$

θ_c - Cone angle

r - distance from vertex of cone

It is developed. Appendix 1 shows that use of spherical polar coordinate system yield same result for thin boundary layer. The various terms of this series are split into universal functions, which are independent of prescribed conditions namely, cone angle, angle of attack, free stream condition etc. The leading term is nonlinear and remaining equations form a recursive set of equations, which are integrated from the surface to

the edge of the boundary layer by using Runge-Kutta method on I.B.M. 7044 Computer with extended precision facility. The values of these functions are tabulated upto six decimal places without rounding off the values. The effect of the prescribed conditions appears in the coefficients of these universal functions. Thus once these tables are available, computation of various dynamic and thermodynamic characteristics of the flow can be done by simple algebraic manipulations. These universal functions are tabulated in Appendix 3.

The computed results for two particular cases show that as thickness parameter increases, there is an increase in skin friction along the generator. But there is a decrease in contribution of incidence in skin friction as thickness parameter increases. Expressions for coefficient of friction and displacement thickness are derived and can be used for the particular case. There are certain limitations of this work also. These limitations are as follows:

- (i) Viscous-inviscid interaction has been neglected.
- (ii) Though the boundary layer is considered thick, θ -momentum equation has been neglected. It does not affect the analysis upto the terms of order α , but once terms of order α^2 or higher are considered, θ -momentum equations should also be considered. This equation is

$$\frac{\partial p}{\partial \theta} = \rho w^2 \cot \theta$$

(iii) Results upto terms of α & ξ only are evaluated, that is only two terms of the series have been considered. Within this approximation, the pressure gradient is favourable in the circumferential direction. As such one should not expect to approach the separation line with the present analysis. In order to include the terms of order ξ^2 and higher, Taylor expansion of $\sin \theta$ should have terms of similar order in $(\theta - \theta_c)$.

(iv) At large angle of attack, near the zone of separation, vortex is shed into the inviscid zone, thus modifying the inviscid flow around the cone. In this case this analysis will not hold. To date, no analytical or experimental work is available to predict the inviscid flow, taking into account the shedding of the vortex into the inviscid zone.

Review of the Past Work

In reference (1) Maccoll has fitted isentropic conical flow to a conical shock, cone being at zero incidence. Due to conical nature of the flow and circumferential symmetry, the three dimensional equations of motion are reduced to one of ordinary non-linear boundary value problem. This equation

is to be solved numerically. Boundary conditions are provided by Rankine-Hugnoit relation across the shock. At the shock and on the surface normal velocity is zero.

In reference (2) Kopal has tabulated, the numerical solution to the equation given by Maccol (1), for various semi-vertex cone angle and various free stream Mach number. In this table, the values of radial and normal velocity components are presented as function of angle θ for a given value of the semi-vertex cone angle, θ_c , and Mach number, M_∞ . These tables also give surface velocity on the cone, shock wave angle and drag coefficient as a function of cone angle and free stream Mach number.

In reference (3) Stone has dealt with the problem of cone at small angles of attack in supersonic stream. The effect of the angle of attack is considered to be a perturbation over the basic solution of Maccoll (1) for the case of zero angle of attack. In this reference the linear terms in angle of attack α are considered. The resulting equations are simplified using the equations of zero incidence case. These resulting equations are to be integrated numerically. The uniqueness of the solution to the approximation taken is also proved, under the assumption that flow properties and their derivatives depend continuously on the angle of attack α .

The equations are integrated starting from the conditions at the shock wave for the symmetric flow until the conditions on the cone are satisfied, that is normal velocity component becomes zero for $\theta = \theta_c$.

In reference (4) Kopal has tabulated the numerical solution of the equations given by Stone (3). The coefficients of α in velocity components, u , v and w , pressure and density are tabulated for a series of semi-vertex cone angle and free stream Mach numbers. It has been found that axial force component does not change from its value in symmetric flow but there exists some normal force component. This is zero in case of zero incidence. These axial and normal force coefficients are also tabulated in this reference.

In reference (5) Stone has extended the analysis of reference (3) to include the terms of second order in angle of attack α and derived the equations governing the coefficients of α^2 in the expansions of velocity components u , v and w , pressure and density. But in deriving these relations, terms of the order of α^3 and $\frac{\alpha^3}{v}$ are neglected. Since normal velocity v becomes zero near the surface, the equations are not valid near the surface of the cone. Boundary conditions are also derived in similar manner. These equations contain singularity in the sense that few terms have normal velocity v in the denominator, which goes to zero as cone surface is reached.

This singularity has been taken care of, by making certain substitutions.

The numerical solution of equations derived by Stone (5), are tabulated by Kopal in reference (6). In these tables various coefficients are tabulated as a function of θ for various values of the free stream Mach number and semi-vertex cone angle. The coefficients in expressions of velocity are referred to maximum velocity while coefficients of pressure and density are referred to their corresponding values at zero angle of attack. These tables also give corresponding shock wave angle, axial force coefficient and normal force coefficient.

In reference (7) Ferri has improved upon Stone's (3) result upto terms of order α and has pointed out that the form of the solution chosen by Stone does not satisfy entropy conservation equation at the surface of the cone. Since cone surface forms a stream surface, the entropy on the surface of the cone is constant but Stone's solution gives variable entropy on the surface of the cone. In this reference asymmetric conical flow has been studied and it has been shown that there must exist singular points in the plane of symmetry. At these singular points entropy is discontinuous. This singularity exists at the point where the circumferential velocity has negative circumferential gradient. Ferri has shown that in most of the regions stream lines are radial and near the surface of the

cone these stream lines move circumferentially and converge at the leeward plane of symmetry. Since each stream-line has different entropy, there is singularity in entropy at leeward plane of symmetry. Also there is a region near the surface of the cone, where the entropy varies significantly. This region has been termed as 'Vortical' layer by Ferri. This vortical layer affects the derivatives of velocity component of zero and first order near the surface of the cone. The term $\frac{\partial S}{\partial \theta}$, which were taken to be zero in Stone's work, are of the order of α in the vortical layer. In this layer it affects the value of $\frac{\partial p}{\partial \theta}$, by quantities of the order of α and pressure by the quantities of the order of $\frac{\phi}{\alpha^2}$. It has also been shown in this reference that for determination of the pressure, complete Bernaulli equation should be used. The pressure distribution calculated in this manner, compares well with experimental analysis.

In reference (8) Young and Siska developed the equations for flow properties in a region bounded by a cone at a large angle of attack and its attached shock wave for the use of tabulation of Kopal (2,4,6). In Reference (4,6), the coefficients of α in the expansion of the velocity components, pressure and density are tabulated, but the boundary conditions are formulated for the conical flow field at zero angle of attack case. Thus while using Kopal table this point need be

taken care of. The equation to correct the values of flow properties are derived in two ways, one by assuming that each intermediate conical surface still remains conical and is rotated by an angle of attack α , and the other by assuming that intermediate conical surface are distorted linearly in a shape from that of solid cone to that of shock wave at an angle of attack. These equations are derived with respect to the wind axes. Equations for the cone surface characteristics e.g. C_d , C_L etc. are also derived with respect to the body axes. Thus this reference improves upon the work of Kopal (4,6), so as to satisfy boundary conditions more accurately.

In Kopal tables (4,6), results are tabulated with respect to wind axes, and Young and Siska (8) have given formulae to use those tabulations in a proper manner the axes still being the wind axes. Only cone surface characteristics are derived in body axis system. In reference (9) Robert and Riley have given the formulae similar to the one given by Young and Siska, but with respect to the body axes. Thus using Kopal table one can get flow properties at a point whose coordinates with respect to the body axes are known. For the derivation it is assumed that the intermediate surfaces are yawed with ^{respect to} solid cone and remain circular cones. The relations for first order and second order terms in α are separately derived. Computed results show good agreement with experimental result even for

$\alpha > \theta_c$. This has been pointed out that there is an error in tabulation in the values of the perturbation in circumferential velocities.

$$y_{\text{correct}} = - (y \text{ from table}) - (2 x / \sin \theta)$$

In reference (10), Willett extended the analysis of Ferri (7) to the terms of order of α^2 . Ferri (7) gave correction to the solution given by Stone (3), Kopal (4) for the presence of vortical layer. Willett has given the equations for correction to Stone (5), Kopal (6) results, due to the presence of vortical layer. In this reference components of velocity on the surface of the cone u and w , pressure and density are evaluated, using Kopal (4,6) and Robert and Riley (9). Thus the flow properties are obtained in body axis system. These relations are derived by assuming that entropy on the cone surface is constant and equals to the entropy of the fluid in windward plane of symmetry. It is also assumed that pressure distribution is correctly given by Stone (5) to the second order. In the derivation of these relations it is assumed that normal velocity is zero. Hence formulae are valid on the surface of cone only and not in the flow field. Experimental results show that the entropy variation with angle of attack is correct upto $\alpha = 20^\circ$ for semi-vertex cone angle $\theta_c = 15^\circ$ and Mach number 3.53. These results on the surface of cone can be used as the boundary

conditions at the edge of boundary layer on the surface of the cone.

In reference (11) Bulakh has extended Stone's (3,5) results inside the vortical layer. The solution inside vortical layer upto the accuracy of α is obtained. This solution reduces to the Stone's results outside the vortical layer. It is also shown that derivatives of entropy, radial and circumferential velocity with respect to polar angle

θ becomes infinity at the surface of the cone. In Stone's (3,5) solution there is a logarithmic singularity in entropy if series is terminated upto α^2 , but if series is carried upto infinity i.e. all the terms in α^n , (n - a natural number) are considered, such logarithmic singularity disappears. This is shown by taking general solution of the entropy conservation equation near the surface of the cone. Though logarithmic singularity is shown to disappear when all the terms in α^n are taken, any numerical work will still have this problem. This reference also proves the assumption of Willett about the pressure on the cone and the entropy jump analytically.

In reference (12) Cheng solved the problem of hypersonic flow around the cone at an angle of attack.

Cheng considered two parameters, one the limiting density ratio across shock wave $\frac{Y-1}{Y+1}$, and other being the angle of attack. The form of solution is same as that of Stone (3,5) except for terms corresponding to the ^{new} parameter density ratio, $\frac{Y-1}{Y+1}$. Cheng gave analytical solution upto the first order terms in density ratio and angle of attack. Expressions for circumferential velocity and pressure are given upto second order approximation also. The derivative of the lift coefficient with respect to angle of attack agrees well with Kopal (4) values. Analytical expression for entropy distribution near the surface of cone is given. First order correction to pressure, density and radial velocity are given by assuming that the singularity does not affect leading approximations of normal and circumferential velocity v & w . These corrected results show that the effect in pressure is in third order only and in the normal and circumferential velocity it is of the second order.

In reference (13) Munson solved the problem of the cone at an angle of attack using the technique of matched asymptotic expansions. Outer expansion is equivalent to Stone's (5) expansion. The inner expansion, which is valid in thin vortical layer near the body describes flow properties in the vortical layer. In the inner expansion coordinate θ has been changed to θ^α in order to take care of logarithmic

perturbation in density. These two expansions are matched asymptotically and then combined to give uniformly valid solution throughout the flow field bounded by cone and attached shock wave. This uniformly valid solution is given both for first order and second order terms separately. It is also shown that pressure does not change inside the vortical layer. He also shows that upto the second order the entropy singularity still remains on the surface of cone and does not go into the fluid.

In reference (14) Babenko et.al discussed numerical method of solving the Euler's equation with proper boundary conditions. A difference scheme for solving the problem of three dimensional flow has been set up. The stability of the method of solving these difference equations is also considered. The method is applied to conical flow equations and equations are solved numerically for various values of angle of attack, Mach number, and semi vertex cone angle. For solving the equations for a given angle of attack, first the equations are solved for zero angle of attack, and then given a small angle of attack $\Delta\alpha$, computation is repeated by taking zero angle of attack solution as basic data. This process is repeated till the required angle of attack is achieved. This process also required some movement along the generator to establish the conical nature of the flow. The results are

tabulated as a function of $\zeta = (\theta - \theta_c) / (\theta - \theta_s)$, where θ_s shock wave inclination and ϕ , the azimuthal angle, for various Mach numbers, angle of attack and semi vertex angle. Inclination of shock wave for each azimuthal angle is also tabulated. Calculation also shows that when Mach number and angle of attack are kept constant and semi-vertex cone angle is increased, shock wave is nearest to the cone in the windward plane of symmetry and later becomes nearest to the cone in the leeward plane of symmetry. The results of computation show that for small angles of attack variation of velocity component with respect to ζ is nearly linear but as angle of attack is increased it becomes more and more nonlinear, while in the analysis of Stone (3,5), this dependence is same for all angles of attack. These tables can be directly used for finding the flow variables for a given tabulated case. But for untabulated case one has to interpolate the results in order to get the flow properties and it is difficult to say what interpolation rule should be used.

In reference (15) Moore has derived the three dimensional boundary layer equations on cone for conical flow. These equations were derived using boundary layer equations in cylindrical polar coordinates and then transforming these equations using Howarth transformation, Mangler's transformation and Blaussiu~~m~~ transformation.

In reference (16) Moore has analysed the laminar boundary layer on a right circular cone at an angle of attack in a supersonic stream. The outer solution to inviscid flow is taken from Kopal (4). Moore considered that for small angles of attack, the boundary layer quantities differ slightly from the corresponding quantities in the flow in case of zero angle of attack. These perturbation quantities are assumed to be of the same form as the outer inviscid flow. The system of equations governing these perturbation quantities is solved to yield the effect of small angles of attack on the velocity profiles, skin friction and boundary layer thickness etc. Actually the rate of change of these quantities with respect to angle of attack are evaluated at zero angle of attack. It has been shown that if we take the case of $\alpha/\theta_c \gg 1$, we get the equations for the compressible viscous flow about a yawed infinite cylinder.

In reference (17, 18) Moore has analysed the problem of laminar boundary layer on a right circular cone at large angle of attack to a supersonic stream, in the plane of symmetry only. It is shown that in the windward plane of symmetry boundary layer becomes thinner when angle of attack increases, but in the leeward plane of symmetry analysis fails to give unique solutions except for the small angle of attack. Beyond a certain critical angle of attack boundary layer flow does

not exist at all. The ratio of this critical angle of attack to the cone semi-vertex angle is given as a function of Mach number. This non-existence of solution on the leeward side indicate a possible separation in the leeward plane of symmetry.

In reference (19) Probestien and Elliot considered the problem of transverse curvature effects in compressible axially symmetric laminar boundary layer flow. In this reference the thickness of the boundary layer is assumed to be comparable to the transverse curvature of the body. The transverse curvature effects are characterised by the parameter which is essentially the ratio of the local boundary layer thickness to the local transverse body radius. Modified Mangler's transformation is used to change the boundary layer equation with terms transverse curvature to almost Cartesian form. The analysis is mainly concerned with the case of transverse curvature parameter being nearly or less than unity. The velocity and temperature are expressed as a power series in transverse curvature and problem is solved for the case of power law bodies, both compressible and incompressible flow and exponentially growing body. The zeroth approximation gives the Mangler's result and higher order approximation modifies the result to include the effect of transverse curvature. The first order analysis for the case of cone and cylinder with zero

pressure gradient shows appreciable change in skin friction and heat transfer rate. This change keeps on increasing with Mach number at the edge of the boundary layer.

In reference (20) Reshotko extended the analysis of Moore (17) for the case of non-insulated surfaces. The boundary layer equations are specialised to the plane of symmetry and are solved numerically. In the plane of symmetry equations become ordinary differential equations. In this analysis boundary layer is assumed to be thin compared to transverse radius of curvature of the cone and ratio of specific heats is taken to be constant. While solving the differential equations in leeward plane of symmetry, it was noted that except for very small angles of attack either the solution is indeterminate or non-existent. It was found that for the case of Prandtl number $Pr = 1$, velocity and temperature profiles $(\frac{T-T_w}{T_o-T_w})$ are same. The circumferential velocity profile exceeds the external circumferential velocity. It is noticed that heat transfer increases significantly with angle of attack for a given free stream Mach number and cone semi-vertex angle. For free stream Mach number of 3.1 and cone semi-vertex angle $\theta_c = 5^\circ$, heat transfer is more than twice at an angle of attack 8° as compared to heat transfer at zero angle of attack. The heat transfer coefficient changes faster for almost insulated

case than for cooled wall case. In this reference method is given to extend the analysis to very large angle of attack using the results of case of yawed infinite cylinder.

In reference (21) Vvedenskaya solved the problem of infinite circular cone at an angle of attack, in a viscous heat conducting fluid. Using finite difference method, self-similar solutions of boundary layer equations are computed. Boundary layer is considered thin compared with ^{radius of} transverse curvature of the body. In this reference after similarity transformation, similarity variable is scaled so as to have the value unity at the edge. The equations are first solved in the plane of symmetry and then in the meridian planes away from the plane of symmetry. Equations are considered to be initial value problem in the circumferential variable. The values of the variable at the edge are taken from Babenko et al (14). It was found that for small angles of attack solution of equations was smooth over the whole surface and the solution matched with ^{the} that solution in the plane of symmetry in the leeward side. The boundary layer also grew monotonically from windward plane of symmetry to leeward plane of symmetry. Heat transfer and friction decreased monotonically with ϕ . But for larger angles of attack ($\alpha > 2.5^\circ$ for $\theta_c = 10^\circ$; $\alpha \geq 5^\circ$ for $\theta_c = 20^\circ$) smooth solution was not possible and circumferential derivatives of velocity components u, w and temperature T did not go to zero

at leeward plane of symmetry. Thus there was a discontinuity in first derivative at leeward plane of symmetry. In such cases it was not possible to solve equations in the leeward plane of symmetry. The displacement thickness on leeward plane of symmetry is several times larger than that on the windward plane of symmetry. For $M_\infty = 5$, and temperature of the body being 500°K , displacement thickness changed from 0.8 on windward side to 5.1 on leeward side, for $\theta_c = 10^\circ$ and $\alpha = 7.5^\circ$. For the same cone when angle of attack was 2.5° it changed from 1.2 to 3.3. The circumferential derivative of heat transfer first increases with α and then decreases at leeward plane of symmetry.

In reference (22) Dwyer computed compressible laminar boundary layer flow over a sharp cone at an angle of attack slightly greater than semi-vortex-cone angle. The boundary layer equation after using similarity, Howarth transformation are solved numerically. These equations are solved as an initial value problem in circumferential variable, and boundary value problem in similarity variable η . Boundary layer is considered thin compared to the ^{radius of} transverse curvature. For boundary conditions at the edge, the result of Munson's (13) work has been taken. For initial condition in ϕ , boundary layer equations were solved in windward plane of symmetry by quasi-linearisation technique. Then boundary layer equations were solved by the

finite difference technique developed by Blottner (24), after some modifications. Nonlinear terms were evaluated at previous station in ϕ . Momentum and energy equations were decoupled between ϕ grid locations by evaluating dependent variables at the previous station. The continuity equation was written in integral form and solved numerically. Steps in ϕ were reduced till convergence in velocity and enthalpy was obtained. Computed results show that in most of the regions relative heat transfer that is actual to zero angle of attack case agree for small α with experimental value if second order expansions for inviscid flow are used. But as the angle of attack is increased the experimental value deviates from computed value. It has been found that beyond a certain angle of attack first order inviscid theory gives serious errors. It is also shown that as angle of attack increases beyond the cone semi-vertex angle, second order expansion of Munson (13) gives inadequate boundary conditions, as the boundary layer structure comes out to be incorrect both ⁱⁿqualitative and quantitative way on the leeward side.

In reference (23) Boerick has done work almost similar to Dwyer (22). In reference (22), reference quantities were arbitrary. While in this case radial and circumferential velocities are normalised with respect to their respective edge velocities. Enthalpy is also normalised with respect to the

edge value. In reference (22) circumferential coordinate is the actual angle ϕ , while in this case it is $\phi \sin \theta_c$. In the leeward plane of symmetry, in order to avoid the numerical difficulties due to vortical singularity, the circumferential coordinate is changed so as to eliminate the singularity from the equations. In the plane of symmetry equations were solved by the 'method of accelerated successive replacements' proposed by Lieberstien (25) and applied to boundary layer problems by Lew (26) and Storm. (27). Blottner method was used for solving equations away from plane of symmetry. The computed results were within 6% of the experimental value for relative heat transfer, when calculations are based on the experimental pressure distributions. In the leeward plane of symmetry error is more than that at other meridinal planes.

CHAPTER 2
GENERAL ANALYSIS

2.1 Formulation

Boundary layer equations in spherical polar coordinate are as follows:

$$\frac{\partial}{\partial r} (r^2 \sin \theta \bar{\rho} \bar{u}) + \frac{\partial}{\partial \theta} (r \sin \theta \bar{\rho} \bar{v}) + \frac{\partial}{\partial \phi} (r \bar{\rho} \bar{w}) = 0 \quad (2.1.1)$$

$$\bar{u} \frac{\partial \bar{u}}{\partial r} + \frac{\bar{v}}{r} \frac{\partial \bar{u}}{\partial \theta} + \frac{\bar{w}}{r \sin \theta} \frac{\partial \bar{u}}{\partial \phi} - \frac{\bar{w}^2}{r} = - \frac{1}{\bar{\rho}} \frac{\partial \bar{p}}{\partial r} + \frac{1}{\bar{\rho} r \sin \theta} \frac{\partial}{\partial \theta} \left(\frac{\mu}{r} \sin \theta \frac{\partial \bar{u}}{\partial \theta} \right) \quad (2.1.2)$$

$$\bar{u} \frac{\partial \bar{w}}{\partial r} + \frac{\bar{v}}{r} \frac{\partial \bar{w}}{\partial \theta} + \frac{\bar{w}}{r \sin \theta} \frac{\partial \bar{w}}{\partial \phi} + \frac{\bar{u}\bar{w}}{r} = - \frac{1}{\bar{\rho} r \sin \theta} \frac{\partial \bar{p}}{\partial \phi} + \frac{1}{\bar{\rho} r \sin \theta} \frac{\partial}{\partial \theta} \left(\frac{\mu}{r} \sin \theta \frac{\partial \bar{w}}{\partial \theta} \right) \quad (2.1.3)$$

and for the case of Prandtl No. $Pr = 1$, energy equation becomes

$$\bar{H}_o = \frac{1}{2} \bar{u}^2 + \frac{1}{2} \bar{w}^2 + \frac{\gamma}{\gamma-1} \frac{\bar{p}}{\bar{\rho}} \quad (2.1.4)$$

Boundary conditions

$$\begin{aligned} \text{at } \theta = \theta_c & \quad \bar{u} = 0 = \bar{v} = \bar{w} \\ \text{at edge} & \quad \bar{u} \rightarrow \bar{u}_e, \bar{w} \rightarrow \bar{w}_e \end{aligned} \quad \left. \right\} \quad (2.1.5)$$

Non-dimensionalising the variables with respect to the inviscid flow quantities on the surface of cone at zero incidence.

$$\begin{aligned} R = \frac{r}{L}, \quad u = \frac{\bar{u}}{\bar{u}_0}, \quad w = \frac{\bar{w}}{\bar{u}_0} \\ \theta = \sqrt{\frac{Re_L}{C_0}} (\theta - \theta_c), \quad v = \sqrt{\frac{Re_L}{C_0}} \frac{\bar{v}}{\bar{u}_0} \\ \rho = \frac{\bar{\rho}}{\bar{\rho}_0}, \quad p = \frac{\bar{p}}{\bar{\rho}_0 \bar{u}_0^2}, \quad H_0 = 2 \frac{\bar{H}_0}{\bar{u}_0^2} \end{aligned} \quad (2.1.6)$$

and using linear viscosity law

$$\mu = \mu_0 C_0 \frac{T}{T_0} \quad (2.1.7)$$

where

\bar{u}_0 - velocity at the surface of cone at zero incidence in inviscid flow.

$\bar{\rho}_0$ - density at the surface of cone at zero incidence in inviscid flow.

T_0 - temperature at the surface of cone at zero incidence
in inviscid flow.

$$Re_T = \frac{\rho_0 \bar{u}_0 L}{\mu_0}, \text{ Reynold number}$$

L - representative length

C_0 - Chapman Rubisen constant

the equations (2.1.1) to (2.1.4) and boundary conditions
(2.1.5) transform to

$$\frac{\partial}{\partial R} (R^2 \sin \theta \rho u) + \frac{\partial}{\partial \theta} (R \sin \theta \rho v) + \frac{\partial}{\partial \phi} (R \rho w) = 0 \quad (2.1.8)$$

$$u \frac{\partial u}{\partial R} + \frac{v}{R} \frac{\partial v}{\partial \theta} + \frac{w}{R \sin \theta} \frac{\partial u}{\partial \phi} - \frac{w^2}{R} = - \frac{1}{\rho} \frac{\partial p}{\partial R}$$

$$+ \frac{1}{\rho R^2 \sin \theta} \frac{\partial}{\partial \theta} \left(\frac{T}{T_0} \sin \theta \frac{\partial u}{\partial \theta} \right) \quad (2.1.9)$$

$$u \frac{\partial w}{\partial R} + \frac{v}{R} \frac{\partial w}{\partial \theta} + \frac{w}{R \sin \theta} \frac{\partial w}{\partial \phi} + \frac{uw}{R} = - \frac{1}{\rho R \sin \theta} \frac{\partial p}{\partial \phi}$$

$$+ \frac{1}{\rho R^2 \sin \theta} \frac{\partial}{\partial \theta} \left(\frac{T}{T_0} \sin \theta \frac{\partial w}{\partial \theta} \right) \quad (2.1.10)$$

$$H_0 = u^2 + w^2 + \frac{2\gamma}{\gamma-1} \frac{p}{\rho} \quad (2.1.11)$$

Boundary conditions

$$\begin{aligned} \text{at } \theta = 0 & \quad u = 0 = v = w \\ \text{at edge} & \quad u \rightarrow u_e; w \rightarrow w_e \end{aligned} \quad (2.1.12)$$

Using stream functions Ψ and χ such that

$$\begin{aligned} \Psi_\theta &= R^2 \sin \theta \rho u \\ \chi_0 &= R \rho w \end{aligned} \quad (2.1.13)$$

and

$$\Psi_R + \chi_\phi = -R \sin \theta v$$

and taking Taylor's expansion of $\sin \theta$ around θ_c upto two terms

$$\begin{aligned} \sin \theta &= \sin \theta_c (1 + \cot \theta_c (\theta - \theta_c)) \\ &= \sin \theta_c (1 + \beta \theta) \end{aligned} \quad (2.1.14)$$

$$\text{where } \beta = \cot \theta_c \sqrt{\frac{C_o}{Re_L}} \quad (2.1.15)$$

Equations (2.1.8) to (2.1.11) and boundary conditions (2.1.12) transform to

$$\frac{\Psi_0}{\rho R^2 \sin \theta_c} \left\{ \frac{\Psi_0}{\rho R^2 \sin \theta_c} (1 - \beta \theta) \right\}_R - \frac{(\Psi_R + X_0)}{\rho R^2 \sin \theta_c}$$

$$\left\{ \frac{\Psi_0 (1 - \beta \theta)}{\rho R^2 \sin \theta_c} \right\}_\theta + \frac{X_0}{\rho R^2 \sin \theta_c} \left\{ \frac{\Psi_0 (1 - \beta \theta)}{\rho R^2 \sin \theta_c} \right\} \phi$$

$$- \frac{(X_0)^2}{\rho^2 R^3} (1 + \beta \theta) = - \frac{1}{\rho} \frac{\partial p}{\partial R} (1 + \beta \theta) + \frac{1}{\rho R^2} \frac{\partial}{\partial \theta}$$

$$\left[\frac{T}{T_0} (1 + \beta \theta) \left\{ \frac{\Psi_0 (1 - \beta \theta)}{\rho R^2 \sin \theta_c} \right\}_\theta \right] \quad (2.1.16)$$

$$\frac{\Psi_0}{\rho R^2 \sin \theta_c} \left(\frac{X_0}{\rho R} \right)_R - \frac{\Psi_R + X_0}{\rho R^2 \sin \theta_c} \left(\frac{X_0}{\rho R} \right)_\theta + \frac{X_0}{\rho R^2 \sin \theta_c} \left(\frac{X_0}{\rho R} \right) \phi$$

$$+ \frac{\Psi_0 X_0}{\rho^2 R^4 \sin \theta_c} = - \frac{1}{\rho R \sin \theta_c} \frac{\partial p}{\partial \phi}$$

$$+ \frac{1}{\rho R^2} \frac{\partial}{\partial \theta} \left\{ \frac{T}{T_0} (1 + \beta \theta) \left(\frac{X_0}{\rho R} \right)_\theta \right\} \quad (2.1.17)$$

and

$$H_0 = \left\{ \frac{\Psi_0}{\rho R^2 \sin \theta_c} \right\}^2 (1 - \beta \theta)^2 + \left(\frac{X_0}{\rho R} \right)^2 + \frac{2\gamma}{\gamma-1} \frac{p}{\rho} \quad (2.1.18)$$

Boundary Conditions

$$\text{at } \theta = 0 \quad \Psi_0 = X_0 = \Psi_R = \phi = 0$$

$$\text{at edge} \quad \frac{\Psi_0}{\rho R^2 \sin \theta_c} (1 - \beta \theta) \rightarrow u_e, \quad \frac{X_0}{\rho R} \rightarrow w_e \quad (2.1.19)$$

It is known that the boundary layer thickness varies as the reciprocal of the square-root of Reynolds number and in case of cone transverse curvature varies directly with R , the distance from the vertex taking the projection of both the boundary layer thickness and the radius of transverse curvature on the plane normal to the axis of cone, one has

$$\xi = \frac{\text{boundary layer thickness}}{\text{radius of transverse curvature}}$$

$$= \frac{\cot \theta_c}{\sqrt{R}} \sqrt{\frac{C_0}{Re_L}}$$

$$\xi = \frac{\beta}{\sqrt{R}} \quad (2.1.20)$$

Now making similarity transformation from (R, θ, ϕ) to (ξ, η, ϕ) such that

$$\xi = \frac{\beta}{\sqrt{R}}$$

$$\eta = \sqrt{\frac{2}{3}} R \left(\frac{p}{p_0}\right)^{-\frac{1}{2}} \int_0^\theta \rho d\theta$$

$$\phi = \phi$$

and

$$\psi = \sqrt{\frac{2}{3}} R^{3/2} \left(\frac{p}{p_0}\right)^{\frac{1}{2}} \sin \theta_c \bar{f}(\xi, \eta, \phi)$$

$$\chi = \sqrt{\frac{2}{3}} R \left(\frac{p}{p_0}\right)^{\frac{1}{2}} g(\xi, \eta, \phi)$$

(2.1.21)

One gets from the Equations (2.1.16) - (2.1.18), after making use of conical nature of outer inviscid flow, the following equations

$$\left\{ -\bar{f} \bar{f}_{\eta\eta} - \frac{2}{3} \frac{g \phi \bar{f}_{\eta\eta}}{\sin \theta_c} - \frac{g p \phi}{3 \sin \theta_c p} \bar{f}_{\eta\eta} + \frac{2}{3} \frac{g \eta \bar{f}_{\eta\phi}}{\sin \theta_c} - \frac{2}{3} g^2 \eta \right. \\ \left. - \frac{\bar{f}}{\bar{f}_{\eta\eta}} \right\} + \xi \left\{ - \frac{\bar{f} \eta \bar{f}_{\eta\xi}}{\frac{2}{3}} + \frac{1}{3} \sqrt{\frac{2}{3}} \bar{f}_{\eta}^2 \left(\frac{p}{p_0}\right)^{\frac{1}{2}} \int_0^1 \frac{1}{\rho} d\rho + \frac{\bar{f} \xi \bar{f}_{\eta\eta}}{\frac{2}{3}} \right. \\ \left. + \sqrt{\frac{2}{3}} \bar{f} \bar{f}_{\eta\eta} \left(\frac{p}{p_0}\right)^{\frac{1}{2}} \int_0^1 \frac{1}{\rho} d\rho + \sqrt{\frac{2}{3}} \frac{\bar{f} \bar{f}_{\eta\eta}}{\rho} \left(\frac{p}{p_0}\right)^{1/2} \right. \\ \left. + \left(\frac{2}{3}\right)^{3/2} \frac{g \phi}{\sin \theta_c} \bar{f}_{\eta\eta} \left(\frac{p}{p_0}\right)^{1/2} \int_0^1 \frac{1}{\rho} d\rho + \left(\frac{2}{3}\right)^{3/2} \frac{g \phi}{\sin \theta_c} \frac{\bar{f} \eta}{\rho} \left(\frac{p}{p_0}\right)^{1/2} \right\}$$

$$\begin{aligned}
& + \left(\frac{2}{3}\right)^{3/2} \frac{g \bar{f} \eta \eta}{2 \sin \theta_c} \frac{p_\phi}{p} \left(\frac{p}{p_0}\right)^{1/2} \int_0^\eta \frac{1}{\rho} d\eta + \left(\frac{2}{3}\right)^{3/2} \frac{g \bar{f} \eta}{2 \sin \theta_c} \frac{p_\phi}{p} \left(\frac{p}{p_0}\right)^{1/2} \\
& - \left(\frac{2}{3}\right)^{3/2} \frac{g \eta \bar{f} \eta \phi}{\sin \theta_c} \left(\frac{p}{p_0}\right)^{1/2} \int_0^\eta \frac{1}{\rho} d\eta - \frac{1}{2} \left(\frac{2}{3}\right)^{3/2} \frac{g \eta \bar{f} \eta}{\sin \theta_c} \left(\frac{p_\phi}{p}\right) \left(\frac{p}{p_0}\right)^{1/2} \\
& \int_0^\eta \frac{1}{\rho} d\eta - \left(\frac{2}{3}\right)^{3/2} \left(\frac{p}{p_0}\right)^{1/2} \frac{g \eta \bar{f} \eta}{\sin \theta_c} \left(\int_0^\eta \frac{1}{\rho} d\eta\right)_\phi \\
& - \left(\frac{2}{3}\right)^{3/2} g_\eta^2 \left(\frac{p}{p_0}\right)^{1/2} \int_0^\eta \frac{1}{\rho} d\eta + \frac{2}{3} \left(\frac{p}{p_0}\right)^{1/2} \frac{f \eta \eta}{\rho} \\
& + \sqrt{\frac{2}{3}} \left(\frac{p}{p_0}\right)^{1/2} \bar{f} \eta \left(\frac{1}{\rho}\right)_\eta \Big\} = 0 \quad (2.1.22)
\end{aligned}$$

$$\begin{aligned}
& \left\{ - \bar{f} g \eta \eta - \frac{2}{3} \frac{g_\phi g \eta \eta}{\sin \theta_c} - \frac{1}{3} \frac{g}{\sin \theta_c} \frac{p_\phi}{p} g \eta \eta + \frac{2}{3} \frac{g \eta}{\sin \theta_c} g \eta \phi \right. \\
& \left. + \frac{2}{3} g \eta \bar{f} \eta + \frac{2}{3} \frac{p_\phi}{p \sin \theta_c} - \frac{g}{\eta \eta \eta} \right\} + \xi \left\{ - \frac{\bar{f} \eta g \eta \xi}{3} + \frac{1}{3} \bar{f} \xi g \eta \eta \right. \\
& \left. - \sqrt{\frac{2}{3}} \left(\frac{p}{p_0}\right)^{1/2} g \eta \eta \int_0^\eta \frac{1}{\rho} d\eta - \sqrt{\frac{2}{3}} \left(\frac{p}{p_0}\right)^{1/2} \frac{g \eta \eta}{\rho} \right\} = 0 \quad (2.1.23)
\end{aligned}$$

$$(H_0 - \bar{f}^2 \eta - g_\eta^2 - \frac{2\gamma}{\gamma-1} \frac{p}{\rho}) + 2\xi \sqrt{\frac{2}{3}} \left(\frac{p}{p_0}\right)^{1/2} \left(\int_0^\eta \frac{1}{\rho} d\eta\right) \bar{f}^2 \eta = 0 \quad (2.1.24)$$

using (2.1.21), boundary conditions (2.1.19) becomes

Boundary conditions

$$\left. \begin{array}{l} \text{at } \eta = 0 \quad \bar{f}_\eta = g_\eta = \bar{f} = \bar{f}_\xi = g_\phi = g = 0 \\ \text{at } \eta \rightarrow \infty \quad \bar{f}_\eta \left(1 - \sqrt{\frac{2}{3}} \xi \left(\frac{p}{p_0} \right)^{1/2} \int_0^\eta \frac{1}{\rho} d\eta \right) = u_e \\ g_\eta \rightarrow w_e \end{array} \right\} \quad (2.1.25)$$

In Equation (2.1.22) and Equation (2.1.24) terms of the order ξ^2 are neglected because Taylor series expansion of $\sin \theta$ is taken upto two terms, that is

$$\sin \theta = \sin \theta_c (1 + \cot \theta_c (\theta - \theta_c))$$

$$= \sin \theta_c (1 + \beta_0) ; \text{ and from (2.1.21)}$$

$$\theta = \sqrt{\frac{2}{3}} \xi \left(\frac{p}{p_0} \right)^{1/2} \int_0^\eta \frac{1}{\rho} d\eta$$

θ involves the terms in ξ and hence, unless the higher order terms in Taylor series expansion of $\sin \theta$ are considered, one should not consider the higher order terms in ξ in the above equations.

Since the boundary condition on \bar{f}_η as $\eta \rightarrow \infty$ is a complicated one and difficult to satisfy while solving the equation numerically, the following substitution is used in order to simplify the boundary condition.

$$\bar{f} = f + \sqrt{\frac{2}{3}} \xi \left(\frac{p}{p_0}\right)^{1/2} \left(f \int_0^\eta \frac{1}{P} d\eta - \int_0^\eta \frac{f}{P} d\eta \right) \quad (2.1.26)$$

substituting (2.1.26) into Equations (2.1.22) to (2.1.24) and neglecting terms of ξ^2 , one gets

$$\left\{ -f \frac{f}{\eta\eta} - \frac{2}{3} \frac{g\phi}{\sin \theta_c} f_{\eta\eta} - \frac{g}{3} \frac{p\phi}{\sin \theta_c} f_{\eta\eta} + \frac{2}{3} \frac{g\eta f\eta \phi}{\sin \theta_c} - \frac{2}{3} g\eta^2 \right. \\ \left. - f_{\eta\eta\eta\eta} \right\} + \xi \left\{ - \left(\frac{2}{3}\right)^{3/2} \left(\frac{p}{p_0}\right)^{1/2} f \frac{f}{\eta\eta} \int_0^\eta \frac{d\eta}{P} \right. \\ \left. + \left(\frac{2}{3}\right)^{3/2} \left(\frac{p}{p_0}\right)^{1/2} f_{\eta\eta} \int_0^\eta \frac{f}{P} \frac{d\eta}{P} + \right. \\ \left. - \sqrt{\frac{2}{3}} \left(\frac{p}{p_0}\right)^{1/2} f_{\eta\eta\eta\eta} \int_0^\eta \frac{\eta}{P} \frac{d\eta}{P} - \sqrt{\frac{2}{3}} \left(\frac{p}{p_0}\right)^{1/2} \frac{f\eta\eta}{P} - \frac{1}{3} f\eta f\eta \xi \right. \\ \left. - \frac{1}{3} \sqrt{\frac{2}{3}} \frac{g\eta f\eta}{\sin \theta_c} \frac{p\phi}{P} \left(\frac{p}{p_0}\right)^{1/2} \int_0^\eta \frac{\eta}{P} \frac{d\eta}{P} - \left(\frac{2}{3}\right)^{3/2} g\eta^2 \left(\frac{p}{p_0}\right)^{1/2} \int_0^\eta \frac{\eta d\eta}{P} \right\} = 0 \quad (2.1.27)$$

$$\left\{ -f g_{\eta\eta} - \frac{2}{3} \frac{g\phi}{\sin \theta_c} g_{\eta\eta} - \frac{1}{3} \frac{g}{\sin \theta_c} \frac{p\phi}{P} g_{\eta\eta} + \frac{2}{3} \frac{g\eta g\eta \phi}{\sin \theta_c} \right. \\ \left. + \frac{2}{3} g\eta f\eta + \frac{2}{3} \frac{p\phi}{P \sin \theta_c} \eta\eta\eta \right\} + \xi \left\{ \frac{4}{3} \sqrt{\frac{2}{3}} \left(\frac{p}{p_0}\right)^{1/2} g_{\eta\eta} \left(f \int_0^\eta \frac{\eta}{P} \frac{d\eta}{P} \right. \right. \\ \left. \left. - \int_0^\eta \frac{f}{P} d\eta \right) + \left(\frac{2}{3}\right)^{3/2} \left(\frac{p}{p_0}\right)^{1/2} g\eta f\eta \int_0^\eta \frac{\eta}{P} \frac{d\eta}{P} - \frac{1}{3} f\eta g\eta \xi \right\}$$

$$+ \frac{1}{3} g \eta \eta f \xi - \sqrt{\frac{2}{3}} \left(\frac{p}{p_0}\right)^{1/2} g \eta \eta \eta \left\{ \frac{\eta d\eta}{\rho} - \sqrt{\frac{2}{3}} \left(\frac{p}{p_0}\right)^{1/2} \frac{g \eta \eta}{\rho} \right\} = 0 \quad (2.1.28)$$

$$H_0 = f \eta^2 + g \eta^2 + \frac{2\gamma}{\gamma-1} \frac{p}{\rho} \quad (2.1.29)$$

Using (2.1.26) boundary conditions become

$$\begin{aligned} \text{at } \eta = 0 \quad f_\eta &= g_\eta = f = f_\xi = g_\phi = g = 0 \\ \text{at } \eta \rightarrow \infty \quad f_\eta &\rightarrow u_e \\ g_\eta &\rightarrow w_e \end{aligned} \quad (2.1.30)$$

2.2 Series Expansion of Stream Functions

Assuming that flow variables f , g and ρ can be expressed as a power series in ξ , the thickness parameter, one can write

$$\rho = \rho_0 + \xi \rho_1 + \xi^2 \rho_2 + \dots$$

$$f = f_0 + \xi f_1 + \xi^2 f_2 + \dots \quad (2.2.1)$$

$$g = g_0 + \xi g_1 + \xi^2 g_2 + \dots$$

Here ρ_0 , f_0 , g_0 , ρ_1 , f_1 , g_1 etc. are functions of η and ϕ alone.

Substituting (2.2.1) in (2.1.27) to (2.1.29) and separating the coefficients of like powers of ξ one gets following equations.

$$f_0 f_0 \eta \eta + \frac{2}{3 \sin \theta_c} g_0 \phi f_0 \eta \eta + \frac{g_0 f_0 \eta \eta}{3 \sin \theta_c} \frac{p_\phi}{p}$$

$$- \frac{2}{3 \sin \theta_c} g_0 \eta f_0 \eta \phi + \frac{2}{3} g_0 \eta^2 + f_0 \eta \eta \eta = 0 \quad (2.2.2)$$

$$- f_0 f_1 \eta \eta - \left\{ \left(\frac{2}{3} \right)^{3/2} \left(\frac{p}{p_0} \right)^{1/2} f_0 f_0 \eta \eta \int \frac{1}{P_0} d\eta \right\}$$

$$- \left(\frac{2}{3} \right)^{3/2} \left(\frac{p}{p_0} \right)^{1/2} f_0 \eta \eta \int_0^\infty \frac{\eta}{P_0} d\eta + \frac{2}{3} f_0 \eta \eta f_1 \right\}$$

$$- \frac{2}{3 \sin \theta_c} (g_1 \phi f_0 \eta \eta + f_1 \eta \eta g_0 \phi) - \frac{p_\phi}{3 \sin \theta_c p} (g_1 f_0 \eta \eta +$$

$$g_0 f_1 \eta \eta) + \frac{2}{3 \sin \theta_c} (g_1 \eta f_0 \eta \phi + g_0 \eta f_1 \eta \phi) - \frac{4}{3} g_0 \eta \epsilon_1 \eta$$

$$- \sqrt{\frac{2}{3}} \left(\frac{p}{p_0} \right)^{1/2} f_0 \eta \eta \eta \int_0^\infty \frac{1}{P_0} d\eta - \sqrt{\frac{2}{3}} \left(\frac{p}{p_0} \right)^{1/2} \frac{f_0 \eta \eta}{P_0} - f_1 \eta \eta \eta$$

$$- \frac{1}{3} f_0 \eta f_1 \eta - \left(\frac{2}{3} \right)^{3/2} g_0^2 \left(\frac{p}{p_0} \right)^{1/2} \int_0^\infty \frac{1}{P_0} d\eta = 0 \quad (2.2.3)$$

$$f_0 g_0 \eta \eta + \frac{2}{3 \sin \theta_c} g_0 \phi g_0 \eta \eta + \frac{1}{3 \sin \theta_c} \frac{p_\phi}{p} g_0 g_0 \eta \eta$$

$$- \frac{2}{3 \sin \theta_c} g_0 \eta g_0 \eta \phi - \frac{2}{3} g_0 \eta f_0 \eta - \frac{2}{3} \frac{p_\phi}{P_0 \sin \theta_c} + g_0 \eta \eta \eta = 0$$

$$(2.2.4)$$

$$\begin{aligned}
 & - \left\{ f_0 g_1 \eta \eta + \left(\frac{2}{3}\right)^{3/2} \left(\frac{p}{p_0}\right)^{1/2} f_0 g_0 \eta \eta \int \frac{1}{\rho_0} d\eta \right. \\
 & - \left. \left(\frac{2}{3}\right)^{3/2} \left(\frac{p}{p_0}\right)^{1/2} g_0 \eta \eta \int \frac{f_0}{\rho_0} d\eta + \frac{2}{3} f_1 g_0 \eta \eta \right\} \\
 & - \frac{2}{3 \sin \theta_c} (g_{1\phi} g_0 \eta \eta + g_{0\phi} g_1 \eta \eta) - \frac{1}{3 \sin \theta_c} \frac{p_\phi}{p} (g_0 g_1 \eta \eta \\
 & + g_1 g_0 \eta \eta) + \frac{2}{3 \sin \theta_c} (g_{0\eta} g_{1\eta} \phi + g_{1\eta} g_{0\eta} \phi) + \frac{2}{3} (g_{1\eta} f_0 \eta \\
 & + \sqrt{\frac{2}{3}} \left(\frac{p}{p_0}\right)^{1/2} g_{0\eta} f_{0\eta} \int \frac{1}{\rho_0} d\eta + g_{0\eta} f_{1\eta}) - \frac{2}{3} \frac{p_\phi}{\sin \theta_c} \frac{\rho_1}{\rho_0^2} \\
 & - g_1 \eta \eta \eta - \frac{1}{3} f_{0\eta} g_{1\eta} - \sqrt{\frac{2}{3}} \left(\frac{p}{p_0}\right)^{1/2} g_{0\eta} \eta \int \frac{1}{\rho_0} d\eta \\
 & - \sqrt{\frac{2}{3}} \left(\frac{p}{p_0}\right)^{1/2} \frac{g_0 \eta \eta}{\rho_0} = 0 \quad (2.2.5) \\
 H_0 & = f_{0\eta}^2 - g_{0\eta}^2 - \frac{2\gamma}{\gamma-1} \frac{p}{\rho_0} = 0 \quad (2.2.6) \\
 f_{0\eta} f_{1\eta} + g_{0\eta} g_{1\eta} - \frac{\gamma}{\gamma-1} p \frac{\rho_1}{\rho_0^2} & = 0 \quad (2.2.7)
 \end{aligned}$$

Boundary conditions

$$\begin{aligned}
 \text{at } \eta = 0 \quad f_0 &= f_1 = f_{0\eta} = f_{1\eta} = g_0 = g_1 = g_{0\phi} = \\
 & g_{1\phi} = g_{0\eta} = g_{1\eta} = 0
 \end{aligned}$$

$$\begin{aligned}
 \text{at } \eta \rightarrow \infty \quad f_{0\eta} &\rightarrow u_e, \quad f_{1\eta} \rightarrow 0 \\
 g_{0\eta} &\rightarrow w_e, \quad g_{1\eta} \rightarrow 0
 \end{aligned} \quad (2.2.8)$$

Now Equations (2.2.2), (2.2.4) and (2.2.6) should be solved for the case of thickness parameter ξ being zero. In order to include the effect of ξ , Equations (2.2.3), (2.2.5) and (2.2.7) should be solved using the solution of Equations (2.2.2), (2.2.4) and (2.2.6). Equations (2.2.6) and (2.2.7) are to be used to eliminate ρ_0 and ρ_1 from Equations (2.2.2), (2.2.3), (2.2.4) and (2.2.5).

Outer inviscid flow for the case of small angle of attack is given by

$$\begin{aligned}
 u_e &= 1 + \alpha x \cos \phi \\
 w_e &= \alpha y \sin \phi \\
 \rho_e &= 1 + \alpha z \cos \phi \\
 \frac{p}{p_0} &= 1 + \alpha \lambda \cos \phi
 \end{aligned} \tag{2.2.9}$$

Expanding the stream functions and density f_0 , g_0 , f_1 , g_1 , ρ_0 and ρ_1 in the similar form one has

$$\begin{aligned}
 f_0 &= f_{00} + \alpha x \cos \phi f_{01} \\
 g_0 &= \alpha y \sin \phi g_{01} \\
 \rho_0 &= \rho_{00} + \alpha z \cos \phi \rho_{01}
 \end{aligned} \tag{2.2.10}$$

$$\begin{aligned}
 \text{and } f_1 &= f_{10} + \alpha x \cos \phi f_{11} \\
 g_1 &= \alpha y \sin \phi g_{11} \\
 \rho_1 &= \rho_{10} + \alpha z \cos \phi \rho_{11}
 \end{aligned} \tag{2.2.11}$$

Here f_{00} , f_{01} , g_{01} , ρ_{00} , ρ_{01} , f_{10} , f_{11} , g_{11} , ρ_{10} , ρ_{11} are functions of η alone. From Equation (2.2.9) one gets

$$\begin{aligned}
 \frac{p}{p_0} &= 1 + \alpha \lambda \cos \phi \\
 \text{and } \frac{p\phi}{p} &= -\alpha \lambda \sin \phi
 \end{aligned} \tag{2.2.12}$$

neglecting the terms of α^2 and higher order.

Substituting Equations (2.2.10) and (2.2.12) in Equations (2.2.2), (2.2.4) and (2.2.6) after neglecting terms of α^2 and higher order and collecting the terms of like powers of α one gets

$$f_{00} f_{00} \eta \eta + f_{00} \eta \eta \eta \eta = 0 \tag{2.2.13}$$

$$f_{01} \eta \eta \eta \eta + f_{00} f_{01} \eta \eta + f_{00} \eta \eta f_{10} = -\frac{2}{3} \frac{y}{x \sin \theta_c} g_{01} f_{00} \eta \eta \tag{2.2.14}$$

$$g_{01} \eta \eta \eta \eta + f_{00} g_{01} \eta \eta - \frac{2}{3} f_{00} \eta g_{01} \eta = -\frac{2}{3} \frac{\lambda y}{y x \sin \theta_c} \frac{p_0}{\rho_{00}} \tag{2.2.15}$$

$$H_0 - f_{00}^2 \eta - \frac{2\gamma}{\gamma-1} \frac{p_0}{\rho_{00}} = 0 \quad (2.2.16)$$

and

$$\frac{\gamma}{\gamma-1} \frac{p_0}{\rho_{00}} \left(\frac{\lambda}{x} - \frac{z}{x} - \frac{p_{01}}{\rho_{00}} \right) + f_{01} \eta f_{00} \eta = 0 \quad (2.2.17)$$

Boundary Conditions using (2.40) in (2.38) gives

$$\text{at } \eta = 0 \quad f_{00} = f_{00}\eta = 0 \quad \text{at } \eta \rightarrow \infty \quad f_{00}\eta \rightarrow 1 \quad (2.2.18)$$

$$\text{at } \eta = 0 \quad f_{01} = f_{01}\eta = 0 \quad \text{at } \eta \rightarrow \infty \quad f_{01}\eta \rightarrow 1 \quad (2.2.19)$$

$$\text{at } \eta = 0 \quad g_{01} = g_{01}\eta = 0 \quad \text{at } \eta \rightarrow \infty \quad g_{01}\eta \rightarrow 1 \quad (2.2.20)$$

Now substituting Equations (2.2.10), (2.2.11), (2.2.12) and (2.2.13) into (2.2.3), (2.2.5) and (2.2.7) and collecting the coefficients of like powers of α , one gets

$$\begin{aligned} f_{10} \eta \eta \eta + f_{00} f_{10} \eta \eta + \frac{1}{3} f_{00} \eta f_{10} \eta + \frac{2}{3} f_{00} \eta \eta f_{10} \\ = - \frac{1}{3} \sqrt{\frac{2}{3}} f_{00} \eta \eta \eta \int \frac{1}{\rho_{00}} d\eta + \left(\frac{2}{3} \right)^{3/2} f_{00} \eta \eta \int \frac{f_{00}}{\rho_{00}} d\eta \\ - \sqrt{\frac{2}{3}} \frac{f_{00}}{\rho_{00}} \end{aligned} \quad (2.2.21)$$

$$\begin{aligned}
& f_{11}\eta\eta\eta + f_{00}f_{11}\eta\eta + \frac{1}{3}f_{00}\eta f_{11}\eta + \frac{2}{3}f_{00}\eta\eta f_{11} \\
& = -f_{01}f_{10}\eta - \left(\frac{2}{3}\right)^{3/2} \left\{ \frac{\lambda}{4x} f_{00}\eta\eta\eta + f_{00}\eta\eta f_{01} + \frac{3}{2}f_{01}\eta\eta\eta \right\} \int \frac{\eta d\eta}{\rho_{00}} \\
& + \sqrt{\frac{2}{3}} \frac{z}{3x} f_{00}\eta\eta\eta \int \frac{\rho_{01}}{\rho_{00}}^2 d\eta + \left(\frac{2}{3}\right)^{3/2} \left\{ \frac{\lambda}{2x} f_{00}\eta\eta + f_{01}\eta\eta \right\} \int \frac{\eta f_{00}}{\rho_{00}} d\eta \\
& + \left(\frac{2}{3}\right)^{3/2} f_{00}\eta\eta \int \frac{f_{01}}{\rho_{00}} d\eta - \left(\frac{2}{3}\right)^{3/2} f_{00}\eta\eta \int \frac{z}{x} \frac{\eta f_{00}}{\rho_{00}} \frac{\rho_{01}}{\rho_{00}} d\eta \\
& - \frac{2}{3}f_{01}f_{10} - \frac{2}{3} \frac{1}{\sin \theta_c} \frac{y}{x} (f_{00}\eta\eta g_{11} + f_{10}\eta\eta g_{01}) - \frac{1}{3}f_{10}\eta f_{01}\eta \\
& - \sqrt{\frac{2}{3}} \left\{ \frac{\lambda}{2x} \frac{f_{00}\eta\eta}{\rho_{00}} + \frac{f_{01}\eta\eta}{\rho_{00}} - \frac{z}{x} \frac{f_{00}\eta\eta \rho_{01}}{\rho_{00}}^2 \right\} \quad (2.2.22)
\end{aligned}$$

$$\begin{aligned}
& g_{11}\eta\eta\eta + f_{00}g_{11}\eta\eta - \frac{1}{3}f_{00}\eta g_{11}\eta \\
& = -\left(\frac{2}{3}\right)^{3/2} f_{00}g_{01}\eta\eta \int \frac{\eta}{\rho_{00}} \frac{d\eta}{\rho_{00}} + \left(\frac{2}{3}\right)^{3/2} g_{01}\eta\eta \int \frac{\eta}{\rho_{00}} \frac{f_{00}}{\rho_{00}} d\eta - \frac{2}{3}f_{10}g_{01} \\
& + \left(\frac{2}{3}\right)^{3/2} g_{01}\eta f_{00}\eta \int \frac{\eta}{\rho_{00}} \frac{d\eta}{\rho_{00}} + \frac{2}{3} \frac{\lambda p_0}{y \sin \theta_c} \frac{\rho_{10}}{\rho_{00}}^2 + \frac{2}{3}g_{01}\eta f_{10}\eta \\
& - \sqrt{\frac{2}{3}} g_{01}\eta\eta\eta \int \frac{\eta}{\rho_{00}} \frac{d\eta}{\rho_{00}} - \sqrt{\frac{2}{3}} \frac{g_{01}\eta\eta\eta}{\rho_{00}} \quad (2.2.23)
\end{aligned}$$

$$f_{00}\eta f_{01}\eta - \frac{\gamma}{\gamma-1} \frac{p_0 \rho_{10}}{\rho_{00}}^2 = 0 \quad (2.2.24)$$

$$f_{00}\eta f_{11}\eta + f_{01}\eta f_{10}\eta - \frac{\gamma}{\gamma-1} p_0 \frac{\rho_{10}}{\rho_{00}^2} \left(\frac{\lambda}{x} + \frac{z}{x} \frac{\rho_{11}}{\rho_{00}} - \frac{2z}{x} \frac{\rho_{01}}{\rho_{00}} \right) = 0 \quad (2.2.25)$$

Boundary Conditions

Using (2.2.11 and 2.2.8) one gets

$$\text{at } \eta = 0 \quad f_{10} = f_{10}\eta = 0 \quad \text{at } \eta \rightarrow \infty \quad f_{10}\eta \rightarrow 0 \quad (2.2.26)$$

$$\text{at } \eta = 0 \quad f_{11} = f_{11}\eta = 0 \quad \text{at } \eta \rightarrow \infty \quad f_{11}\eta \rightarrow 0 \quad (2.2.27)$$

$$\text{at } \eta = 0 \quad g_{11} = g_{11}\eta = 0 \quad \text{at } \eta \rightarrow \infty \quad g_{11}\eta \rightarrow 0 \quad (2.2.28)$$

These equations are ordinary differential equation of third order. These are to be solved numerically in order to find the solution to original problem.

2.3 Reduction of Stream Functions into Universal Functions

Since the equations governing the stream functions f_{01} , g_{01} , f_{10} , f_{11} , g_{11} are non-homogeneous and non-homogeneous part contains the terms like x , z , λ etc., which depend upon the particular flow situation, these need be solved for each particular case of free stream mach number, semi-vertex cone angle and angle of attack. In order to avoid this problem of solving these differential equations each time separately the stream functions are broken into universal functions. The differential equations governing these universal functions are independent of the particular flow situations, and their linear combination

gives these stream functions. In this linear combination the coefficients of the universal functions depend upon the particular flow situations. Thus the problem is to be solved only once and any particular case can be derived by taking the proper linear combination of these universal functions.

Letting

$$f_{\infty} = F_{\infty} \quad (2.3.1)$$

from (2.2.13) and (2.2.18) one gets

$$F_{\infty}''' + F_{\infty} F_{\infty}'' = 0 \quad (2.3.2)$$

Boundary conditions

$$\begin{aligned} \text{at } \eta = 0 \quad F_{\infty} = F'_{\infty} = 0 \\ \text{at } \eta \rightarrow \infty \quad F'_{\infty} \rightarrow 1 \end{aligned} \quad (2.3.3)$$

(Here prime denotes differentiation with respect to η).

From the definition of p one has

$$p = \frac{\bar{p}}{\bar{\rho}_0 \bar{U}_0^2}$$

At the edge of boundary layer for zero incidence one has

$$\begin{aligned} p_0 &= \frac{\bar{p}_0}{\bar{\rho}_{\infty} \bar{U}_0^2} \\ &= \frac{1}{\gamma M^2} \end{aligned} \quad (2.3.4)$$

and from (2.2.16) one has

$$H_0 = 1 + \frac{2}{(\gamma-1) M_0^2} \quad (2.3.5)$$

where M_0 is the Mach number at the edge of the boundary layer in the case of zero angle of attack.

Now letting

$$g_{01} = F_{00} + (1 + \frac{\gamma-1}{2} M_0^2) G_{011} \quad (2.3.6)$$

from (2.2.15), (2.2.16) and (2.3.6) one gets

$$G_{011}''' + F_{00} G_{011}'' - \frac{2}{3} F_{00}' G_{011}' = - \frac{2}{3} (1 - F_{00}^2) \quad (2.3.7)$$

Boundary conditions

$$\begin{aligned} \text{at } \eta = 0 \quad G_{011} &= G_{011}' = 0 \\ \text{at } \eta \rightarrow \infty \quad G_{011}' &\rightarrow 0 \end{aligned} \quad (2.3.8)$$

Letting

$$\begin{aligned} f_{01} &= - \frac{2}{3} \frac{y}{x \sin \theta_c} F_{00} + (1 + \frac{2}{3} \frac{y}{x \sin \theta_c}) F_{011} \\ &+ \frac{2y}{3x \sin \theta_c} (1 + \frac{\gamma-1}{2} M_0^2) F_{012} \quad (2.3.9) \end{aligned}$$

and after substituting in equations (2.2.14) and (2.3.6)
one gets

$$F_{011}''' + F_{000} F_{011}'' + F_{000}^2 F_{011}' = 0 \quad (2.3.10)$$

Boundary conditions

$$\left. \begin{array}{l} \text{at } \eta = 0 \quad F_{011}' = F_{011}''' = 0 \\ \text{at } \eta \rightarrow \infty \quad F_{011}' \rightarrow 1 \end{array} \right\} \quad (2.3.11)$$

and

$$F_{012}''' + F_{000} F_{012}'' + F_{000}^2 F_{012}' = - F_{000}''' G_{011} \quad (2.3.12)$$

Boundary conditions

$$\left. \begin{array}{l} \text{at } \eta = 0 \quad F_{012}' = F_{012}''' = 0 \\ \text{at } \eta \rightarrow \infty \quad F_{012}' \rightarrow 0 \end{array} \right\} \quad (2.3.13)$$

Similarly, letting

$$f_{10} = F_{101} + (\gamma - 1) M_0^2 F_{102} \quad (2.3.14)$$

and substituting in (2.2.21) and using (2.2.16) and (2.3.2)
one gets

$$\begin{aligned} F_{101}''' + F_{000} F_{101}'' + \frac{1}{3} F_{000}^2 F_{101}' + \frac{2}{3} F_{000}''' F_{101} \\ = \left(\frac{2}{3}\right)^{3/2} F_{000}'' \int_0^\eta F_{000} d\eta - \frac{1}{3} \sqrt{\frac{2}{3}} \eta F_{000}''' - \sqrt{\frac{2}{3}} F_{000}'' \end{aligned} \quad (2.3.15)$$

$$\begin{aligned}
 L(G_{111}) = & - \left(\frac{2}{3}\right)^{3/2} \eta F_{00} (F_{00}'' + G_{011}'') + \left(\frac{2}{3}\right)^{3/2} F_{00}'' \int_0^\eta F_{00} d\eta \\
 & + \left(\frac{2}{3}\right)^{3/2} G_{011}'' \int_0^\eta F_{00} d\eta - \frac{2}{3} (F_{00}'' + G_{011}'') F_{101} \\
 & + \left(\frac{2}{3}\right)^{3/2} \eta F_{00}' (F_{00}'' + G_{011}'') + \frac{2}{3} F_{101}' (F_{00}'' + G_{011}'') \\
 & - \sqrt{\frac{2}{3}} (F_{00}'' + G_{011}'') - \sqrt{\frac{2}{3}} (F_{00}'' + G_{011}'') \quad (2.3.21)
 \end{aligned}$$

Boundary conditions

$$\begin{aligned}
 \text{at } \eta = 0 \quad G_{111} = G_{111}' = 0 \\
 \text{at } \eta \rightarrow \infty \quad G_{111}' \rightarrow 0 \quad (2.3.22)
 \end{aligned}$$

$$\begin{aligned}
 L(G_{112}) = & - \frac{1}{2} \left(\frac{2}{3}\right)^{3/2} F_{00} (F_{00}'' + G_{011}'') (\eta - F_{00} F_{00}' - F_{00}'') \\
 & - \left(\frac{2}{3}\right)^{3/2} \frac{\eta}{2} F_{00} G_{011}'' + \frac{1}{2} \left(\frac{2}{3}\right)^{3/2} (F_{00}'' + G_{011}'') \\
 & \left(\int_0^\eta F_{00} d\eta - \int_0^\eta F_{00} F_{00}'' d\eta \right) + \frac{1}{2} \left(\frac{2}{3}\right)^{3/2} G_{011}'' \int_0^\eta F_{00} d\eta \\
 & - \frac{2}{3} F_{102} (F_{00}''' + G_{011}'') - \frac{1}{3} F_{101} G_{011}'' \\
 & - \frac{1}{2} \left(\frac{2}{3}\right)^{3/2} F_{00}' (F_{00}'' + G_{011}'') (\eta - F_{00} F_{00}' - F_{00}'')
 \end{aligned}$$

$$\begin{aligned}
& + \frac{1}{2} \left(\frac{2}{3}\right)^{3/2} \eta F_{00}^1 G_{011}^1 + \frac{2}{3} F_{00}^1 F_{101}^1 + \frac{2}{3} F_{102}^1 (F_{00}^1 + G_{011}^1) \\
& + \frac{1}{3} F_{101}^1 G_{011}^1 - \frac{1}{2} \sqrt{\frac{2}{3}} (F_{00}^{'''1} + G_{011}^{'''1}) (\eta - F_{00}^1 F_{00}^1 - F_{00}^{''1}) \\
& - \frac{1}{2} \sqrt{\frac{2}{3}} G_{011}^{'''1} - \frac{1}{3} \sqrt{\frac{2}{3}} (G_{011}^{''1} + F_{00}^{''1}) (1 - F_{00}^{12}) - \frac{1}{2} \sqrt{\frac{2}{3}} G_{011}^{''1}
\end{aligned} \tag{2.3.23}$$

Boundary conditions

$$\begin{aligned}
\text{at } \eta = 0 \quad G_{112}^1 = G_{112}^{''1} = 0 \\
\text{at } \eta \rightarrow \infty \quad G_{112}^1 \rightarrow 0
\end{aligned} \tag{2.3.24}$$

and

$$\begin{aligned}
L(G_{113}) = & - \frac{1}{4} \left(\frac{2}{3}\right)^{3/2} F_{00}^1 G_{011}^{''1} (\eta - F_{00}^1 F_{00}^1 - F_{00}^{''1}) \\
& + \frac{1}{4} \left(\frac{2}{3}\right)^{3/2} G_{011}^{''1} \int_0^\eta F_{00}^1 (1 - F_{00}^{12}) d\eta - \frac{1}{3} F_{102}^1 G_{011}^{''1} \\
& + \frac{1}{4} \left(\frac{2}{3}\right)^{3/2} F_{00}^1 G_{011}^1 (\eta - F_{00}^1 F_{00}^1 - F_{00}^{''1}) + \frac{2}{3} F_{00}^1 F_{012}^1 \\
& + \frac{1}{3} G_{011}^1 F_{102}^1 - \frac{1}{4} \sqrt{\frac{2}{3}} G_{011}^{'''1} (\eta - F_{00}^1 F_{00}^1 - F_{00}^{''1}) \\
& - \frac{1}{4} \sqrt{\frac{2}{3}} G_{011}^{''1} (1 - F_{00}^{12})
\end{aligned} \tag{2.3.25}$$

Boundary conditions

$$\left. \begin{array}{l} \text{at } \eta = 0 \quad G_{113} = G'_{113} = 0 \\ \text{at } \eta \rightarrow \infty \quad G'_{113} \rightarrow 0 \end{array} \right\} \quad (2.3.26)$$

$$\begin{aligned} f_{11} = & F_{111} + \frac{y}{x \sin \theta_c} F_{112} + (\gamma - 1) M_0^2 F_{113} \\ & + \frac{y}{x \sin \theta_c} (\gamma - 1) M_0^2 F_{114} + \frac{y}{x \sin \theta_c} (\gamma - 1)^2 M_0^4 F_{115} \\ & + \frac{\lambda}{x} F_{116} + \frac{\lambda}{x} (\gamma - 1) M_0^2 F_{117} \end{aligned} \quad (2.3.27)$$

and

$$L_1 (f) = f''' + F_{00} f'' + \frac{1}{3} F_{00}' f' + \frac{2}{3} F_{00}'' f \quad (2.3.28)$$

and

using (2.3.27), (2.2.22), (2.3.6), (2.3.9), (2.3.14), (2.3.19), (2.2.16), (2.2.17) etc. one gets,

$$\begin{aligned} L_1 (F_{111}) = & - F_{011} F_{101}'' - \left(\frac{2}{3}\right)^{3/2} \eta (F_{00} F_{011}'' + F_{00}'' F_{011}) \\ & - \sqrt{\frac{2}{3}} \eta F_{011}''' + \left(\frac{2}{3}\right)^{3/2} F_{011}'' \int_0^\eta F_{00} d\eta \\ & + \left(\frac{2}{3}\right)^{3/2} F_{00}'' \int_0^\eta F_{011} d\eta - \frac{2}{3} F_{101} F_{011}'' - \frac{1}{3} F_{101}' F_{011} - \sqrt{\frac{2}{3}} F_{011}'' \end{aligned} \quad (2.3.29)$$

Boundary conditions

$$\left. \begin{array}{l} \text{at } \eta = 0 \quad F_{111} = F_{111}^t = 0 \\ \text{at } \eta \rightarrow \infty \quad F_{111}^t \rightarrow 0 \end{array} \right\} \quad (2.3.30)$$

$$\begin{aligned} L_2 (F_{112}) = & - \frac{2}{3} F_{101}^n (F_{011} + F_{012} - F_{00}) - \left(\frac{2}{3}\right)^{5/2} \eta F_{00} (F_{011} \\ & + F_{012} - F_{00}) - \left(\frac{2}{3}\right)^{5/2} \eta F_{00} (F_{011} + F_{012} - F_{00}) \\ & - \left(\frac{2}{3}\right)^{3/2} \eta (F_{011}^n - F_{00}^n + F_{012}^n) \\ & + \left(\frac{2}{3}\right)^{5/2} (F_{011}^n + F_{012}^n - F_{00}^n) \int_0^\eta F_{00} d\eta \\ & + \left(\frac{2}{3}\right)^{5/2} F_{00} \int_0^\eta (F_{011} + F_{012} - F_{00}) d\eta \\ & - \frac{4}{9} F_{101} (F_{011}^n + F_{012}^n - F_{00}^n) - \frac{2}{3} F_{00}^n G_{111} \\ & - \frac{2}{3} F_{00} F_{101}^n - \frac{2}{3} F_{101}^n G_{011} - \frac{2}{9} F_{101} (F_{011}^n + F_{012}^n - F_{00}^n) \\ & - \left(\frac{2}{3}\right)^{3/2} (F_{011}^n + F_{012}^n - F_{00}^n) \end{aligned} \quad (2.3.31)$$

Boundary conditions

$$\left. \begin{array}{l} \text{at } \eta = 0 \quad F_{112} = F_{112}' = 0 \\ \text{at } \eta \rightarrow \infty \quad F_{112}' \rightarrow 0 \end{array} \right\} (2.3.32)$$

$$\begin{aligned} L_1 (F_{113}) = & - F_{102}'' F_{011} - \frac{1}{2} \left(\frac{2}{3}\right)^{3/2} F_{000} F_{011}'' (\eta - F_{000} F_{000}' - F_{000}'') \\ & - \frac{1}{3} \sqrt{\frac{2}{3}} F_{000}'' F_{011} (\eta - F_{000} F_{000}' - F_{000}'') \\ & - \frac{1}{2} \sqrt{\frac{2}{3}} F_{011}''' (\eta - F_{000} F_{000}' - F_{000}'') + \frac{1}{3} \sqrt{\frac{2}{3}} F_{000}''' \int_0^\eta F_{000}' F_{011} d\eta \\ & + \frac{1}{3} \sqrt{\frac{2}{3}} F_{011}'' \int_0^\eta F_{000} (1 - F_{000}'^2) d\eta \\ & + \frac{1}{3} \sqrt{\frac{2}{3}} F_{000}' \int_0^\eta F_{011} (1 - F_{000}'^2) d\eta \\ & - \left(\frac{2}{3}\right)^{3/2} F_{000}'' \int_0^\eta F_{000} F_{000}' F_{011} d\eta - \frac{2}{3} F_{011}'' F_{102} \\ & - \frac{1}{3} F_{011}' F_{102}' - \frac{1}{2} \sqrt{\frac{2}{3}} F_{011}'' (1 - F_{000}'^2) + \sqrt{\frac{2}{3}} F_{000}' F_{011}' F_{000}'' \end{aligned} \quad (2.3.33)$$

Boundary conditions

$$\left. \begin{array}{l} \text{at } \eta = 0 \quad F_{113} = F_{113}' = 0 \\ \text{at } \eta \rightarrow \infty \quad F_{113}' \rightarrow 0 \end{array} \right\} (2.3.34)$$

$$\begin{aligned}
 L_1 (F_{114}) = & \dots + \frac{1}{3} F_{102}'' (F_{011} + F_{012} - F_{00}) - \frac{1}{3} F_{012} F_{101}'' \\
 & - \frac{1}{3} \left(\frac{2}{3}\right)^{3/2} \eta F_{012}'' F_{00} \\
 & - \frac{1}{3} \left(\frac{2}{3}\right)^{3/2} F_{00} (\eta - F_{00} F_{00}' - F_{00}'') (F_{011}'' - F_{00}'' + F_{012}'') \\
 & - \frac{1}{3} \left(\frac{2}{3}\right)^{3/2} \eta F_{00}'' F_{012} \\
 & - \frac{1}{3} \left(\frac{2}{3}\right)^{3/2} F_{00}'' (\eta - F_{00} F_{00}' - F_{00}'') (F_{011}'' - F_{00}'' + F_{012}'') \\
 & - \frac{1}{3} \sqrt{\frac{2}{3}} \eta F_{012}'' \\
 & - \frac{1}{3} \sqrt{\frac{2}{3}} (\lambda - F_{00} F_{00}' - F_{00}'') (F_{011}''' - F_{00}''' + F_{012}''') \\
 & + \frac{1}{3} \left(\frac{2}{3}\right)^{3/2} F_{00}'' \int_0^\eta F_{00}' (F_{011}' - F_{00}' + F_{012}') d\eta \\
 & + \frac{1}{3} \left(\frac{2}{3}\right)^{3/2} (F_{011}'' + F_{012}'' - F_{00}'') \int_0^\eta F_{00} (1 - F_{00}^2) d\eta \\
 & + \frac{1}{3} \left(\frac{2}{3}\right)^{3/2} F_{012}'' \int_0^\eta F_{00} d\eta \\
 & + \frac{1}{3} \left(\frac{2}{3}\right)^{3/2} F_{00}'' \int_0^\eta F_{012} d\eta
 \end{aligned}$$

$$\begin{aligned}
& + \frac{1}{3} \left(\frac{2}{3}\right)^{3/2} F_{00}'' \int_0^\eta (1 - F_{00}'^2) (F_{011} + F_{012} - F_{00}'') d\eta \\
& - \left(\frac{2}{3}\right)^{5/2} F_{00}'' \int_0^\eta F_{00}' F_{00}'' (F_{011}' - F_{00}' + F_{012}') d\eta \\
& - \frac{2}{9} F_{101} F_{012}'' - \frac{2}{3} F_{00}'' G_{112} - \frac{1}{3} G_{011} F_{101}'' \\
& - \frac{4}{9} F_{102} (F_{011}'' + F_{012}'' - F_{00}'') \\
& - \frac{2}{3} (F_{00}'' F_{102} + G_{011} F_{102}'' + \frac{F_{101} G_{011}}{2}) - \frac{1}{9} F_{101}' F_{012}' \\
& - \frac{2}{9} F_{102}' (F_{011}' + F_{012}' - F_{00}') + \left(\frac{2}{3}\right)^{3/2} F_{012}'' \\
& - \left(\frac{2}{3}\right)^{3/2} (1 - F_{00}'^2) (F_{011}'' + F_{012}'' - F_{00}'') \\
& + \left(\frac{2}{3}\right)^{3/2} F_{00}'' F_{00}' (F_{011}' + F_{012}' - F_{00}') \quad (2.3.35)
\end{aligned}$$

Boundary conditions

$$\begin{aligned}
\text{at } \eta = 0 \quad F_{114} = F_{114}' = 0 & \\
\text{at } \eta \rightarrow \infty \quad F_{114}' \rightarrow 0 & \quad \left. \right\} \quad (2.3.36)
\end{aligned}$$

$$\begin{aligned}
 L_1 (F_{115}) = & -\frac{1}{3} F_{012} F_{102}'' - \frac{1}{9} \sqrt{\frac{2}{3}} F_{00} F_{012}'' (\eta - F_{00} F_{00}' - F_{00}'') \\
 & - \left(\frac{2}{3}\right)^{5/2} F_{00}' F_{012} (\eta - F_{00} F_{00}' - F_{00}'') \\
 & - \frac{1}{6} \sqrt{\frac{2}{3}} F_{012}''' (\eta - F_{00} F_{00}' - F_{00}'') \\
 & + \frac{1}{9} \sqrt{\frac{2}{3}} F_{00} \int_0^\eta F_{00}' F_{012} d\eta \\
 & + \frac{1}{6} \left(\frac{2}{3}\right)^{3/2} F_{012}'' \int_0^\eta F_{00} (1 - F_{00}'^2) d\eta \\
 & + \frac{1}{6} \left(\frac{2}{3}\right)^{3/2} F_{00}'' \int_0^\eta F_{012} (1 - F_{00}'^2) d\eta \\
 & - \frac{1}{3} \left(\frac{2}{3}\right)^{3/2} F_{00}'' \int_0^\eta F_{00}' F_{012} d\eta - \frac{2}{9} F_{012}'' F_{102} \\
 & - \frac{2}{3} F_{00}'' G_{113} - \frac{1}{9} F_{012}' F_{102}' - \frac{1}{6} \sqrt{\frac{2}{3}} F_{012}'' (1 - F_{00}'^2) \\
 & + \frac{1}{3} \sqrt{\frac{2}{3}} F_{00}'' F_{00}' F_{012}' \quad (2.3.37)
 \end{aligned}$$

Boundary conditions

$$\begin{aligned}
 \text{at } \eta = 0 \quad F_{115} = F_{115}' = 0 \\
 \text{at } \eta \rightarrow \infty \quad F_{115}' \rightarrow 0
 \end{aligned}
 \quad \left. \right\} \quad (2.3.38)$$

$$L_1 (F_{116}) = + \frac{1}{6} \sqrt{\frac{2}{3}} F_{00}''' - \frac{1}{3} F_{00}'' \int_0^\eta F_{00} d\eta + \frac{1}{2} \sqrt{\frac{2}{3}} F_{00}'' \quad (2.3.39)$$

Boundary conditions

$$\left. \begin{array}{l} \text{at } \eta = 0 \quad F_{116} = F'_{116} = 0 \\ \text{at } \eta \rightarrow \infty \quad F'_{116} \rightarrow 0 \end{array} \right\} \quad (2.3.40)$$

and

$$\begin{aligned} L_1 (F_{117}) = & + \frac{1}{12} \left(\frac{2}{3}\right)^{1/2} F_{00}'' (\eta - F_{00} F_{00}' - F_{00}'') \\ & + \frac{1}{2} \sqrt{\frac{2}{3}} F_{00}''' \int_0^\eta F_{00} (1 - F_{00}'^2) d\eta + \frac{1}{4} \sqrt{\frac{2}{3}} F_{00}''' (1 - F_{00}'^2) \end{aligned} \quad (2.3.41)$$

Boundary conditions

$$\left. \begin{array}{l} \text{at } \eta = 0 \quad F_{117} = F'_{117} = 0 \\ \text{at } \eta \rightarrow \infty \quad F'_{117} \rightarrow 0 \end{array} \right\} \quad (2.3.42)$$

These equations (2.3.1), (2.3.6), (2.3.10), (2.3.12), (2.3.15), (2.3.17), (2.3.21), (2.3.23), (2.3.25), (2.3.29), (2.3.31), (2.3.33), (2.3.35), (2.3.37), (2.3.39) and (2.3.41) are to be solved recursively with proper boundary conditions. Once these equations are solved with proper boundary conditions, one can

get f_{00} , g_{01} , f_{01} , f_{10} , g_{11} and f_{11} and hence f and g for a given particular flow situation, thus giving detailed behaviour of the flow.

These equations are solved numerically by Runge-Kutta Method for solving third order differential equations as given by Collatz (28).

CHAPTER 3

RESULTS

The various boundary layer quantities e.g. skin friction, boundary layer thickness etc. can be evaluated by using Equations (2.2.1), (2.2.10), (2.2.11), (2.3.1), (2.3.6), (2.3.9), (2.3.14), (2.3.19) and (2.3.37) and the universal function tabulated in Appendix 3. The coefficients of these universal function are to be taken from Kopal (2,4). Figure 3 to 12 present the quantities related to velocity profile for two cases, one for semi-vertex cone angle of 5° and free stream Mach number of 8.4925 and other for semi-vertex cone angle of 7.5° and free stream Mach number of 8.0589.

Velocity Profile

Velocity profile for the case zero angle of attack are shown in Figures 3 and 4 for the two cases. Both these figures show that as thickness parameter ξ increases, velocity profile becomes more and more steep near the surface of the cone. This increase in steepness implies increase in skin friction. This increase in the skin friction is also depicted in Figures 7 and 8, in which shear profile is plotted for the two cases. This increase in the shear stress is due to decrease in local Reynold's number as ξ increases, thus increasing

viscous forces in comparison with inertia forces.

Velocity profile in circumferential direction are plotted in Figures 5 and 6 for the two cases. Both these graphs show that circumferential velocity profile becomes less steep with increase in thickness parameter ξ . This implies that skin friction in circumferential direction decreases with increase in ξ . This decrease in the circumferential shear stress is also depicted in Figures 9 and 10. These figures show the shear profile of circumferential direction.

The rate of increment in the meridinal velocity profile due to angle of attack is given by

$$\frac{1}{\cos \phi} \left\{ \frac{\partial}{\partial \alpha} \left(\frac{u}{u_e} \right) \Big|_{\alpha=0} \right\} = x (f_{o1} + \xi f_{11} - f_{oo} - \xi f_{10})$$

This quantity is plotted in Figures 11 and 12 for the two cases. These graphs show that as thickness parameter increases, there is decrease in this rate of increment.

Skin Friction -

The circumferential and the meridinal components of the viscous shear stress at the cone surface are given by

$$Cf_{\phi} = \frac{2}{\bar{\rho}_o \bar{u}_o^2} (\mu \frac{\partial \bar{w}}{\partial \theta})|_{\theta=\theta_c}$$

$$Cf_r = \frac{2}{\bar{\rho}_o \bar{u}_o^2} (\mu \frac{\partial \bar{u}}{\partial \theta})|_{\theta=\theta_c}$$

Making the quantities non-dimensional on the right hand side of these equations one has

$$Cf_{\phi} = 2 \sqrt{\frac{3C_o}{2Re_r}} \left(\frac{p}{p_o}\right)^{\frac{1}{2}} g_{\eta\eta}(0)$$

$$Cf_r = 2 \sqrt{\frac{3}{2} \frac{C_o}{Re_r}} \left(\frac{p}{p_o}\right)^{\frac{1}{2}} f_{\eta\eta}(0)$$

$$\text{where } Re_r = \frac{\bar{\rho}_o \bar{u}_o r}{\mu_o}$$

Using expansions of f and g and making use of tabulated functions one gets

$$Cf_{\phi} = 2 \sqrt{\frac{3}{2} \frac{C_o}{Re_r}} \alpha y \sin \phi \left\{ 1.0836 + 0.3070 (\gamma-1) M_o^2 \right. \\ \left. - 0.8430 \xi - 0.2049 (\gamma-1) M_o^2 \xi - 0.0283 (\gamma-1)^2 \xi M_o^4 \right\}$$

$$\begin{aligned}
 Cf_r &= 2 \sqrt{\frac{3}{2}} \frac{C_o}{Re_r} \left[0.4696 + 0.4989 \xi + 0.2301 (\gamma-1) M_o^2 \xi \right. \\
 &+ \alpha x \cos \phi \left[0.7046 + 0.1930 \frac{\lambda}{x} + 0.0130 \frac{\lambda}{x} \xi \right. \\
 &+ 0.1150 (\gamma-1) M_o^2 \frac{\lambda \xi}{x} \left. + 0.2487 \frac{y}{x \sin \theta_c} \right. \\
 &+ 0.0460 \frac{y}{x \sin \theta_c} (\gamma-1) M_o^2 + 0.5042 \xi \\
 &- 0.9596 - \frac{y \xi}{x \sin \theta_c} - 0.1839 (\gamma-1) M_o^2 \xi \\
 &- 0.2431 \frac{y \xi}{x \sin \theta_c} (\gamma-1) M_o^2 \\
 &\left. - 0.0234 \frac{y \xi}{x \sin \theta_c} (\gamma-1)^2 M_o^4 \right] \}
 \end{aligned}$$

Both of these expressions reduce to result equivalent to that of Moore (16) for $\xi = 0$ and that of Probestien and Elliot (19) for $\alpha = 0$ and to that of Mangler for $\alpha = \xi = 0$.

Boundary Layer Thickness

The boundary layer thickness, when expressed as displacement thickness, associated with the velocities w and u are as follows:

$$\delta_{\phi}^* = \int_0^{\text{edge}} r \left(1 - \frac{\bar{\rho} \bar{w}}{\bar{\rho}_e \bar{w}_e} \right) d\theta$$

$$\delta_r^* = \int_0^{\text{edge}} r \left(1 - \frac{\bar{\rho} \bar{u}}{\bar{\rho}_e \bar{v}_e} \right) d\theta$$

Expressing the quantities in the non-dimensional form on the right hand side of these equations one has

$$\delta_{\phi}^* = \sqrt{\frac{2}{3} \frac{C_o}{Re_r}} \left(\frac{p}{p_o} \right)^{1/2} \int_0^{\infty} \left(\frac{1}{D} - \frac{\bar{\rho}_o}{\bar{\rho}_e} \frac{\bar{u}_o}{\bar{u}_e} w \right) d\eta$$

and

$$\delta_r^* = \sqrt{\frac{2}{3} \frac{C_o}{Re_r}} \left(\frac{p}{p_o} \right)^{1/2} \int_0^{\infty} \left(\frac{1}{D} - \frac{\bar{\rho}_o}{\bar{\rho}_e} \frac{\bar{u}_o}{\bar{u}_e} u \right) d\eta$$

Using the expansions of f and g that is for u and w and integrating with the use of tables one gets

$$\delta_{\phi}^* = \sqrt{\frac{2}{3} \frac{C_o}{Re_r}} \left\{ 0.6518 - 6.8715 \zeta + (\kappa-1) M_o^2 (0.5707 - 2.2929 \zeta) \right. \\ \left. - 0.5237 (\kappa-1) M_o^2 \right\}$$

$$\delta_r^* = \sqrt{\frac{2}{3} \frac{C_o}{Re_r}} [1.2168 + 1.9218 (\kappa-1) M_o^2 +]$$

$$\zeta \left\{ -0.5618 + 0.3734 (\gamma-1) M_0^2 + 0.3367 (\gamma-1)^2 M_0^4 \right\}$$

$$+ \alpha x \cos \phi \left\{ 0.6214 + 0.4924 (\gamma-1) M_0^2 \right.$$

$$- 0.5031 (\gamma-1) M_0^2 \frac{y}{x \sin \theta_c} + 0.1434 (\gamma-1)^2 M_0^4$$

$$- 0.6376 \zeta (\gamma-1) M_0^2 - 4.9899 \frac{y \zeta}{x \sin \theta_c} (\gamma-1) M_0^2$$

$$- 0.0251 (\gamma-1)^2 M_0^2 \zeta - 4.1295 \frac{y \zeta}{x \sin \theta_c} (\gamma-1)^2 M_0^4$$

$$- 0.1243 \frac{y \zeta}{x \sin \theta_c} (\gamma-1)^3 M_0^6 + 0.5480 \frac{\lambda \zeta}{x}$$

$$+ 0.2636 \frac{\lambda \zeta}{x} (\gamma-1) M_0^2 - 0.6941 \frac{y}{x \sin \theta_c} - 0.5505 \zeta$$

$$- 2.7985 \frac{y \zeta}{x \sin \theta_c} + 5.3916 \frac{\lambda}{x} + 0.9609 (\gamma-1) M_0^2 \frac{\lambda}{x}$$

$$- 0.1683 \frac{\lambda \zeta}{x} (\gamma-1)^2 M_0^4 \}]$$

These expressions reduces to the results equivalent to that of Moore for $\zeta = 0$.

It should be noted here that this analysis is valid only in the limit of vanishing angle of attack α and thickness parameter ζ . Actually the terms multiplied by α and ζ

represent the rate of changes with respect to these quantities, evaluated at $\alpha = 0$ and $\xi = 0$ respectively. Whether or not the absolute change for a small finite angle of attack α and thickness parameter ξ can be obtained from this theory depends on the relative magnitude of the effects so computed, rather than on the size of angle of attack α and thickness parameter ξ and depends further on the second and higher order terms in the expressions of f , g etc.

REFERENCES

1. MacColl, J.W.; 'The Conical Shock Wave Formed by a Cone Moving at High Speeds', Proc. Roy. Soc. A.159 (1937) pp 459.
2. Kopal, Z.; 'Table of Supersonic Flow Around Cones', M.I.T., Dept. of Electrical Engg. Center of Analysis, Technical Report 1, Cambridge, Mass. 1947.
3. Stone, A.H.; 'On Supersonic Flow Past Slightly Yawing Cones I', Journal of Mathematics and Physics, Vol.27, 1948, pp 67-81.
4. Kopal, Z.; 'Table of Supersonic Flow Around Yawing Cones', M.I.T., Dept. of Electrical Engg, Centre of Analysis, Technical Report 2, Cambridge, Mass.
5. Stone, A.H.; 'On Supersonic Flow Past Slightly Yawing Cones II', Journal of Maths. and Physics, Vol.30, 1951, pp 203-213.
6. Kopal, Z.; 'Table of Supersonic Flow Around Yawing Cones', M.I.T., Dept. of Electrical Engg., Centre of Analysis, Technical Report 3, Cambridge, Mass.
7. Ferri, A.; 'Supersonic Flow Around Cones at an Angle of Attack', N.A.C.A. T.R. 1045, 1951.

8. Young, G.B.W. and Siska, C.P.; 'Supersonic Flow Around Cones at Large Yaw', Journal of Aeronautical Sciences, Vol. 19, 1952, pp. 111.
9. Roberts, R.C. and Riley, J.D.; 'A Guide to the Use of M.I.T. Cone Tables', Journal of Aeronautical Sciences, Vol. 21, 1954, pp. 336.
10. Willett, J.E.; 'Supersonic Flow at the Surface of Circular Cone at an Angle of Attack', Journal of Aerospace Sciences, Vol. 27, 1960, pp. 907.
11. Bulakh, B.M.; 'Supersonic Flow Around an Inclined Circular Cone', P.M.M., Vol. 26, 1962 (Journal of App. Maths. & Mechanics, pp. 460).
12. Cheng, H.K.; 'Hypersonic Flow Past Yawed Circular Cone and Other Pointed Bodies', Journal of Fluid Mechanics, Vol. 12, 1964, pp. 169.
13. Munson, A.G.; 'The Vortical Layer on an Inclined Cone', Journal of Fluid Mechanics, Vol. 20, 1964, pp. 625.
14. Babenko, K.I.; Voskresenkiy, G.P.; Lyubimov, A.N. and Rusinov, V.V.; 'Three Dimensional Flow of Ideal Gases Around Smooth Bodies', Israel Program for Scientific Translations, Jerusalem, 1968.

22. Dwyer, H.A.; 'Boundary Layer on a Hypersonic Sharp Cone at Small Angle of Attack', A.I.A.A. Journal, Vol. 9, Feb. 1971.
23. Boericke, R.R.; 'The Laminar Boundary Layer on a Cone at Incidence in Supersonic Flow', A.I.A.A. Journal, Vol. 9, March 1971.
24. Blottner, F.; 'Finite Difference Methods of Solution of Boundary Layer Equations', AIAA Journal, Vol.8, Feb. 1970.
25. Lieberstien, H.; 'Course in Numerical Analysis', Harper and Row, New York, 1968.
26. Lew, H.; 'The Use of the Method of Accelerated Successive Replacements for the Solution of Boundary Layer Equations', A.I.A.A. Journal, Vol.6, May 1968.
27. Storm, G.R.; 'Application of the Method of Nonlinear Simultaneous Displacements to General Three-Dimensional Stagnation Point Boundary Layer Equations', A.I.A.A. Paper 68-786, Los-Angles, Calif., 1968.
28. Collatz, L.; 'The Numerical Treatment of Differential Equations', Springer-Verlag, Berlin, Heidelberg, New York, 1966.

APPENDIX 1JUSTIFICATION FOR USING SPHERICAL POLAR COORDINATES

Spherical polar coordinate system is used in place of the usual cylindrical coordinate system in the present work. In order to justify the use of spherical polar coordinate system and corresponding similarity variable analysis of thin boundary layer on a cone at zero angle of attack is performed in coordinate systems and coefficient of friction is compared.

Boundary layer equations in cylindrical polar coordinate system are as follows

$$\frac{\partial}{\partial x} (\bar{\rho} \bar{r} \bar{u}) + \frac{\partial}{\partial y} (\bar{\rho} \bar{r} \bar{u}) = 0 \quad (A.1.1)$$

$$\bar{u} \frac{\partial \bar{u}}{\partial x} + \bar{v} \frac{\partial \bar{u}}{\partial y} = \frac{1}{\bar{\rho}} \frac{\partial}{\partial y} (\bar{\mu} \frac{\partial \bar{u}}{\partial y}) \quad (A.1.2)$$

$$\bar{H} = \text{Const} = \bar{H}_e \quad (A.1.3)$$

It is assumed that Prandtl number is unity and no heat transfer takes place. Outer flow is assumed to be conical in nature.

Boundary conditions

$$\text{at } \bar{y} = 0 \quad \bar{u} = \bar{v} = 0 \quad (A.1.4)$$

$$\text{at } \bar{y} \rightarrow \bar{\delta} \quad \bar{u} \rightarrow \bar{u}_e$$

Non-dimensionalising the variables

$$R = \frac{\bar{r}_0}{L}, \quad x = \bar{x}/L, \quad y = \bar{y}/L \quad \sqrt{\frac{Re_L}{C_0}}$$

$$H = \frac{\bar{H}}{\frac{1}{2} \bar{u}_e^2}, \quad u = \frac{\bar{u}}{\bar{u}_e}, \quad v = \frac{\bar{v}}{\bar{u}_e} \sqrt{\frac{Re_L}{C_0}}, \quad \rho = \frac{\bar{\rho}}{\rho_e} \quad (A.1.5)$$

where L is some given length parameter and C_0 is Chapman-Rubisen constant, one gets

$$\frac{\partial}{\partial x} (\rho R u) + \frac{\partial}{\partial y} (\rho R v) = 0 \quad (A.1.6)$$

$$u \frac{\partial u}{\partial x} + v \frac{\partial u}{\partial y} = \frac{1}{\rho} - \frac{\partial}{\partial y} \left(\frac{T}{T_0} \frac{\partial u}{\partial y} \right) \quad (A.1.7)$$

$$H = H_e \quad (A.1.8)$$

Boundary conditions at

$$y = 0 \quad u = v = 0 \quad (A.1.9)$$

$$y \rightarrow \delta \quad u \rightarrow 1$$

Using stream function Ψ such that

$$\Psi_y = \rho R u \quad (A.1.10)$$

$$\Psi_x = -\rho R v$$

satisfying equation (A.1.6) identically, one gets

$$\left(\frac{\Psi_y}{\rho R}\right) \left(\frac{\Psi_y}{\rho R}\right)_x - \left(\frac{\Psi_x}{\rho R}\right) \left(\frac{\Psi_y}{\rho R}\right)_y = \frac{1}{\rho} \left\{ \frac{T}{T_o} \left(\frac{\Psi_y}{R}\right)_y \right\}_y \quad (A.1.11)$$

Boundary conditions

$$\text{at } y = 0 \quad \Psi_y = \Psi_x = 0 \quad (A.1.12)$$

$$\text{at } y \rightarrow \delta \quad \Psi_y \rightarrow R$$

Using combined Howarth, Mangler and similarly transformation

$$\begin{aligned} \xi &= \int_0^x R^2 dx \\ \eta &= \frac{\int_0^y R \rho dy}{\sqrt{2\xi}} \end{aligned} \quad (A.1.13)$$

and

$$\Psi = \sqrt{2\xi} f(\eta) \quad (A.1.14)$$

one gets

$$ff_{\eta\eta} + f_{\eta\eta\eta} = 0 \quad (A.1.15)$$

Boundary conditions

$$\text{at } \eta = 0 \quad f = f' = 0$$

$$\text{at } \eta \rightarrow \infty \quad f \rightarrow 1$$

$$\} \quad (A.1.16)$$

Now

$$\tau = \bar{\mu} \frac{\partial \bar{u}}{\partial \bar{y}} \quad (\text{A.1.17})$$

$$C_f = \frac{\tau}{\frac{1}{2} \bar{\rho}_e \bar{u}_e^2} = \frac{2 \bar{\mu}}{\bar{\rho}_e \bar{u}_e^2} \frac{\partial \bar{u}}{\partial \bar{y}} \Big|_{\bar{y}=0} \quad (\text{A.1.18})$$

$$\begin{aligned} C_f &= 2 \sqrt{\frac{3}{x}} \sqrt{\frac{C_0}{\text{Re}_L}} f \eta \eta(0) \\ &= 2 \sqrt{\frac{3 C_0}{2 \text{Re}_x}} f \eta \eta(0) \end{aligned} \quad (\text{A.1.19})$$

Boundary layer equations over a cone in spherical polar coordinate system are as follows.

$$\frac{\partial}{\partial \bar{r}} (\bar{r}^2 \sin \theta \bar{\rho} \bar{u}) + \frac{\partial}{\partial \theta} (\bar{r} \sin \theta \bar{\rho} \bar{u}) = 0 \quad (\text{A.1.20})$$

$$\bar{u} \frac{\partial \bar{u}}{\partial \bar{r}} + \frac{\bar{v}}{\bar{r}} \frac{\partial \bar{u}}{\partial \theta} = \frac{1}{\bar{\rho}} \frac{\partial}{\partial \theta} \left(\frac{\mu}{\bar{r}} \frac{\partial \bar{u}}{\partial \theta} \right) \quad (\text{A.1.21})$$

and for Prandtl number equal to unity and no heat transfer case

$$\bar{H} = \bar{H}_e \quad (\text{A.1.22})$$

Boundary conditions

$$\left. \begin{aligned} \text{at } \theta = \theta_e \quad \bar{u} = \bar{v} = 0 \\ \text{at } \theta \rightarrow \text{edge} \quad \bar{u} \rightarrow u_e \end{aligned} \right\} \quad (\text{A.1.23})$$

Non-dimensionalizing the variables

$$R = \frac{\bar{r}}{L}, \quad u = \frac{\bar{u}}{u_e}, \quad \rho = \frac{\bar{\rho}}{\rho_e} \quad (A.1.24)$$

$$H = \frac{1}{2} \frac{\bar{H}}{u_e^2}, \quad \theta = \sqrt{\frac{Re_L}{C_0}} (\theta - \theta_c), \quad v = \sqrt{\frac{Re_L}{C_0}} \frac{\bar{v}}{u_e}$$

$$\frac{\partial}{\partial R} (R^2 \sin \theta \rho u) + \frac{\partial}{\partial \theta} (\rho R \sin \theta v) = 0 \quad (A.1.25)$$

$$u \frac{\partial u}{\partial R} + \frac{v}{R} \frac{\partial u}{\partial \theta} = \frac{1}{\rho R^2} \frac{\partial}{\partial \theta} \left(\frac{T}{T_0} \frac{\partial u}{\partial \theta} \right) \quad (A.1.26)$$

$$H = H_e \quad (A.1.27)$$

Boundary conditions

$$\begin{aligned} \text{at } \theta = 0 \quad & u = v = 0 \\ \text{at } \theta \rightarrow \text{edge} \quad & u \rightarrow 1 \end{aligned} \quad (A.1.28)$$

Using stream function

$$\left. \begin{aligned} \Psi_\theta &= R^2 \sin \theta \rho u \\ \Psi_R &= -R \sin \theta \rho v \end{aligned} \right\} \quad (A.1.29)$$

Since boundary layer is thin it is assumed that $\sin \theta = \sin \theta_c$

then one gets

$$\begin{aligned} \frac{\Psi_0}{\rho R^2 \sin \theta_c} \left(\frac{\Psi_0}{\rho R^2 \sin \theta_c} \right)_R - \frac{\Psi_R}{\rho R^2 \sin \theta_c} \left(\frac{\Psi_0}{\rho R^2 \sin \theta_c} \right)_\theta \\ = \frac{1}{\rho R^2} \frac{\partial}{\partial \theta} \left\{ \frac{T}{T_0} \left(\frac{\Psi_0}{R \sin \theta_c} \right)_\theta \right\} \quad (A.1.30) \end{aligned}$$

Using combined Howarth similarity transformation

$$\xi = R \quad (A.1.31)$$

$$\eta = \sqrt{\frac{3R}{2}} \int_0^\theta \rho d\theta$$

and

$$\Psi = \sqrt{\frac{2}{3}} R^{3/2} \sin \theta_c f(\eta) \quad (A.1.32)$$

one gets

$$ff_{\eta\eta} + f_{\eta\eta\eta} = 0 \quad (A.1.33)$$

Boundary conditions

$$\text{at } \theta = 0 \quad f = f_\theta = 0$$

$$\text{at } \theta \rightarrow \infty \quad f \rightarrow 1$$

$$\left. \right\} \quad (A.1.34)$$

Now Coefficient of friction

$$\begin{aligned} C_f &= \frac{2T}{\rho_e u_e^2} = \frac{2\mu}{\rho_e u_e^2} - \frac{\partial u}{\partial \theta} \Big|_{\theta=\theta_c} \\ &= 2 \sqrt{\frac{3C_0}{2Re_r}} f_{\eta\eta}(0) \quad (A.1.35) \end{aligned}$$

Since equations (A.1.5) and (A.1.34) and their corresponding boundary conditions are same, the value of $f_{\eta\eta}(0)$ are same for both the equations. Now comparison of equations (A.1.19) and (A.1.35) shows that value of coefficient of friction is same in both the cases.

This shows that for thin similar boundary layer over a cone in conical inviscid flow, analysis in any of the coordinate system renders same result.

APPENDIX 2
COMPUTER PROGRAMME FOR SOLVING
DIFFERENTIAL EQUATIONS

ARGUE, THE FOR ,21050000,NAME = D100000 ,24000000
DE 03000000 03,20000000 02, BOTH WITH 01000

10000000,1,110,111,BLOCK100,SHUFFLE,TYPE3,LRL=107,RCT=1,
NAME10000000,NAME20000000,NAME30000000,NAME40000000

TO NAME
DOUBLE PRECISION X,Y,XP,YPP,YPPP,F(30),G(30),H(30),E(30),
1 ALG(30),Y0,YD,YDD,Y20,Y30,Y40,Y50,Y60,Y70,Y80,Y90,Y100,Y110,
2 YK0,YK10,YK20
DOUBLE PRECISION X0,PP0
COMMON X,Y,XP,YPP,YPPP,F(30),G(30),H(30),E(30),
ALG(30),Y0,YD,YDD,Y20,Y30,Y40,Y50,Y60,Y70,Y80,Y90,Y100,Y110

X,Y,XP,YPP,YPPP ARE VALUES OF SIMILARITY VARIABLE ,FUNCTION,
ITS FIRST,SECOND AND THIRD DERIVATIVES RESPECTIVELY FOR THE
CURRENT EQUATION BEING SOLVED

ARRAYS P,Q,R,S,E GIVE VALUES OF SIMILARITY VARIABLE(FUNCTION),2ND
FLOOR, 2ND AND 3RD DERIVATIVES OF PREVIOUS FUNCTIONS SOLVED

AT THE PRESENT LOCATION OF SIMILARITY VARIABLE

ARRAY NAME IS THE NAME OF UNIVERSAL FUNCTION EVALUATED
CALL TIME(1,1,1,1)

1111=2

111=35

110=2

11=1

10=32

PRINT0=11,111

PRINT00=1

1 FORMAT(1111)

2 FORMAT(2,111)

3 FORMAT(3,111)

4E(11,10,2)90T22

PRINT VALUES OF PREVIOUSLY SOLVED FUNCTIONS AND THEIR DERIVATIVES

PRINT=1,111

READ(3,213)NAME(1),G(1),H(1),E(1),F(1),E(1)

WRITE(2,213)NAME(1),G(1),H(1),E(1),F(1),E(1)

23 FORMAT(1X,15,5D24.10)

3 CONTINUE

IF(K.LT.10,110,111)READ(8)AL(1)

IF(K.GT.10)READ(8)(AL(I),I=1,11)

```

READ(3, NAME(NN+1))
N=2.0
DECIDE THE EQUATION TO BE SOLVED AND CORRESPONDING INITIAL
  CONDITIONS
X=0.0
Y=0.0
YD=0.0
GOT0(3,4,5,6,7,8,9,0,8,7,8,8,8,8,8,8,8,7,0,8,0,0,0,0,0,0,0,3,8,
1,8),K
YDP=0.40000
GOT01
YDP=0.0070352760100000000
GOT02
YDP=0.7004812030000000000
GOT03
YDP=0.7002004065354000000
GOT04
  YDP=1.0
GOT05
  YDP=0.0
GOT06(10,11,12,13,14,15,16,17,0,10,0,10,0,10,0,10,0,10,0,10,0,10,
11,0,2,1,0,2,10,0,10,0),K
YDP=1.000/1000
  CALL FUM(YDP,K)
PRINT3, NAME(NN+1), X, Y, YD, YDP, YDP
W11TE(2,2,13)NAME(NN+1), X, Y, YD, YDP, YDP
DC13WK=1,600
RUNGE-KUTTA METHOD FOR THIRD ORDER ORDINARY DIFFERENTIAL EQUAT
X0=X
Y0=Y
V10=H*YD
V20=H/2.*H*YDP
RK1=H/2.*4/3.*H*YDP
X=X0+H/2.
Y=Y0+V10/2.+V20/4.+2RK1/9.
V101=V10+V20+.75*2RK1
YD=V101/H
V201=V20+1.5*RK1
YDP=V201/H*2./H
  CALL FUM(YDP,K)

```

1923, 11, 15 (1947)

DE THE EQUATIONS TO BE SOLVED AND CORRESPONDING INITIAL CONDITIONS.

K
20000

2023 RELEASE UNDER E.O. 14176

2021 RELEASE UNDER E.O. 14176

卷之二

2013-02-22 10:53:57.000000

22=1.2
2110

11-5118 (XBB22-V)

HTO33, NAME(NP+1), X, Y, YD, YDD, YDDD
HTO34, NAME(NP+1), X, Y, YD, YDD, YDDD

13440 = 1,600

2.5-EXTRA METHODS FOR PREDICTING ORDINARY DISEASES: INFERENTIAL STATISTICS

34

1

卷之三

11/2 11/17

7/24/18/8

卷之三

33-V154-V264-35+2K3

2013/11

471-1271

2-924
2-12274

2974/192.76

26 *Environ Biol Fish* (2007) 79–88


```

CONTINUE, JUNIT(100+1)
FORMAT(2,1X,* 202X STARTS *,A5)
FORMAT(2,1X,* 202X FINISH *,A5)
I151=2, KKK
READ(2,103)X,Y,YD,YDD,YDDD
WRITE(2,103)X,Y,YD,YDD,YDDD
CONTINUE
JUNIT102, JUNIT(100+1)
=100+1
T(K,50,1,10,X,50,10) CALL JUNIT(K)
DT012
D0=YD
DT012
D1=YD
CONTINUE
K=2,1
K=1+K/10
K211=1,10
READ(3,103)X,Y,YD,YDD,YDDD
READ(3,103)X,Y,YD,YDD,YDDD
FORMAT(2I3,15,F6.2,6E15.2)
CONTINUE
E(100)KK,10).50.001M=100+0.1
CONTINUE
TOP
PRINT(10,101,X
E2 101,T(2,1X,* 2000000 OUT OF ORDER *,2025.10)
TOP
ND
CONTINUE
SUBROUTINE FIN(3,1)
* SUBROUTINE EVALUATES THIRD DERIVATIVES OF VARIOUS UNIVERSAL
FUNCTIONS
DOUBLE PRECISION X,Y,YD,YDD,YDDD,T,S,P,E,AL
D0
X,Y,YD,YDD,T,S,P,E,AL
D=2./3.
D=DSQRT(22)
CIDE THE EQUATION TO BE SOLVED

```



```

-2./D.*C(5)*E(6))-h./2.*C(5)*(E(3)+E(4)-E(1))
-2./3.*C(2)*(C(3)+C(2))+C(2)/2.*E(5))-2./3.*E(1)*C(2)
-D(5)/7.*D(4)-2./7.*D(5)*(D(3)+D(4)-D(1))-DD**3*E(4)
-DD**3*(C.-D(1)*D(1))*(E(3)+E(4)-E(1)) -C(2)/3.*E(5)
+DD**3*E(1)*D(2)*(D(3)-D(1))
+DD**3*D(1)*D(1) *D(6)
END

FUNCTION F115
-2./3.*C(2)*Y-D(1)/3.*YD-D(1)*YDD-D(4)/3.*E(5)-DD/2.*C(1)
h)*(X-C(3)*D(1)-E(1))-DD**5*E(1)*C(4)*(X-C(1)*D(1)-E(1))
/2.*E(4)*(X-C(1)*D(1)-E(1))+DD/2.*E(1)*AL(11)
**3/2.*E(4)*AL(4)+DD**3/2.*E(1)*AL(12)-DD**3/3.*AL(13)*E(1)
/2.*C(5)*E(4)-2./3.*E(3)*C(2)-D(4)/2.*D(5)
/2.*E(4)*(1,-D(1)*D(1))+DD/3.*E(1)*D(1)*D(4)
END

FUNCTION F116
-2./3.*C(1)*Y-D(1)*YD-D(1)*YDD +DD/3.*X*E(1)+DD/3.
1)*(AL(1)-DD**3*X*AL(1)*E(1)+DD/2.*E(1)-DD**3/2.*X*E(1)
END

FUNCTION F117
-2./3.*E(1)*Y-D(1)/3.*YD-D(1)*YDD
/2.*E(1)*(X-C(1)*D(1)-E(1))+DD/2.*AL(4)*E(1)+DD/3.*AL(4) *E(1)
/2.*E(1)*(1,-D(1)*D(1))
-DD**3/2.*((X-C(1)*D(1)-E(1))* E(1)
END

D
DT
SUBROUTINE DINT(XXXXXX)
DOUBLE PRECISION D(30),C(30),D(30),E(30),AL(30),BL(30)
INTEGRATION OF VARIOUS COMBINATIONS OF FUNCTIONS AND THEIR
DERIVATIVES
END
3
11024
11025
11026
11027
DINT DDD
DDIMAT(2111)
(XXXXXX,EC,10)GOTO50
(1)=1,2
(1)=2,3
501 =1,021

```

```

1000K=3,4
1010D(3,2)*D(K),C(K),D(K),E(K),F(K)
1020CONTINUE
1030L(1)=AL(1)+2.115*(DL(1)+C(1))
1040L(1)=C(1)
1050WRITE(6)AL(1)
1060D(MD(1,10),5E,2)PRINT 0,2,AL(1)
1070CONTINUE
1080ENDIF(L,6)
1090ENDIF(L,3)
1100ENDIF(L,4)
1110CONTINUE
1120I1=1,35
1130L(1)=0.
1140L(1)=0.1
1150CONTINUE
1160D25=LT(SY,D25,76)
1170D231=1,50
1180C2K=1,2
1190D(3,2)*D(K),C(K),D(K),E(K),F(K)
1200PRINT(6X,D231,10)
1210CONTINUE
1220L(1)=AL(1)+2.115*(DL(1)+C(1))
1230L(1)=C(1)
1240L(2)=AL(2)+2.115*(DL(2)+C(3)+C(4)-C(1))
1250L(2)=C(3)+C(4)-C(1)
1260L(3)=AL(3)+2.115*(DL(3)+D(1)*D(3))
1270L(3)=D(1)*D(3)
1280L(4)=AL(4)+2.115*(DL(4)+C(1)*(1.-D(1)*D(1)))
1290DL(4)=C(1)*(1.-D(1)*D(1))
1300L(5)=AL(5)+2.115*(DL(5)+C(3)*(1.-D(1)*D(1)))
1310L(5)=C(3)*(1.-D(3)*D(3))
1320L(6)=AL(6)+2.115*(DL(6)+C(1)*D(1)*D(3))
1330L(6)=C(1)*D(1)*D(3)
1340L(7)=AL(7)+2.115*(DL(7)+D(1)*(D(1)-D(3)-D(4)))
1350L(7)=D(1)*(D(1)-D(3)-D(4))
1360L(8)=AL(8)+2.115*(DL(8)+C(1)*D(1)*(D(3)+D(4)-D(1)))
1370L(8)=C(1)*D(1)*(D(3)+D(4)-D(1))
1380L(9)=AL(9)+2.115*(DL(9)+C(4))
1390L(9)=C(4)

```

```

10)=AL(10)+7.705*(DL(10)+(3,-D(3)*D(1))*(C(3)+C(4)-C(1)))
10)=(1,-D(1)*D(1))*(C(3)+C(4)-C(1))
11)=AL(11)+7.705*(DL(11)+D(1)*D(4))
11)=D(1)*D(4)
12)=AL(12)+7.715*(DL(12)+C(5)*(3,-D(1)*D(1)))
12)=C(5)*(1,-D(1)*D(1))
13)=AL(13)+7.715*(DL(13)+C(7)*D(1)*D(6))
13)=C(1)*D(7)*D(3)
14)=AL(14)+7.715*(DL(14)+C(3))
14)=C(3)
15)=AL(15)+7.715*(DL(15)+C(6))
15)=C(6)
TF(k)(^L(k),k=1,35)
1/2*2^1+1
11,FQ,1)221-T222, (^L(k),k=1,15)
TIME
DELL E h
MP3
MP4 h
MP5

```

TABLE OF UNIVERSAL FUNCTIONS

APPENDIX 3

TABLE I

TABLE OF UNIVERSAL FUNCTION EGQ

三

23

1

13

EIA

TABLE 2

TABLE OF UNIVERSAL FUNCTION 6111

	F	F	F	F	F	F
0.00	0.000000	0.000000	0.000000	0.000000	0.000000	0.000000
0.20	0.111311	0.109497	0.109497	0.102548	0.102548	0.08102
0.40	0.351302	0.349496	0.349496	0.323340	0.323340	0.285763
0.60	0.691302	0.689496	0.689496	0.66653	0.66653	0.595135
0.80	0.931302	0.929496	0.929496	0.902548	0.902548	0.823340
1.00	0.111311	0.109497	0.109497	0.102548	0.102548	0.08102
1.20	0.351302	0.349496	0.349496	0.323340	0.323340	0.285763
1.40	0.691302	0.689496	0.689496	0.66653	0.66653	0.595135
1.60	0.931302	0.929496	0.929496	0.902548	0.902548	0.823340
1.80	0.111311	0.109497	0.109497	0.102548	0.102548	0.08102
2.00	0.351302	0.349496	0.349496	0.323340	0.323340	0.285763
2.20	0.691302	0.689496	0.689496	0.66653	0.66653	0.595135
2.40	0.931302	0.929496	0.929496	0.902548	0.902548	0.823340
2.60	0.111311	0.109497	0.109497	0.102548	0.102548	0.08102
2.80	0.351302	0.349496	0.349496	0.323340	0.323340	0.285763
3.00	0.691302	0.689496	0.689496	0.66653	0.66653	0.595135
3.20	0.931302	0.929496	0.929496	0.902548	0.902548	0.823340
3.40	0.111311	0.109497	0.109497	0.102548	0.102548	0.08102
3.60	0.351302	0.349496	0.349496	0.323340	0.323340	0.285763
3.80	0.691302	0.689496	0.689496	0.66653	0.66653	0.595135
4.00	0.931302	0.929496	0.929496	0.902548	0.902548	0.823340
4.20	0.111311	0.109497	0.109497	0.102548	0.102548	0.08102
4.40	0.351302	0.349496	0.349496	0.323340	0.323340	0.285763
4.60	0.691302	0.689496	0.689496	0.66653	0.66653	0.595135
4.80	0.931302	0.929496	0.929496	0.902548	0.902548	0.823340
5.00	0.111311	0.109497	0.109497	0.102548	0.102548	0.08102
5.20	0.351302	0.349496	0.349496	0.323340	0.323340	0.285763
5.40	0.691302	0.689496	0.689496	0.66653	0.66653	0.595135
5.60	0.931302	0.929496	0.929496	0.902548	0.902548	0.823340
5.80	0.111311	0.109497	0.109497	0.102548	0.102548	0.08102
6.00	0.351302	0.349496	0.349496	0.323340	0.323340	0.285763

ETA E

374 V. I.

1405 441101001718384101 30 378711

TABLE OF INVENTORYSAL EINIGER FESTE

3 27661

TABLE 5
TABLE OF UNIVERSAL FUNCTION F101

ETA	F	F'	F''
0.00	0.000000	0.000000	0.498863
0.20	0.009465	0.002072	0.421656
0.40	0.035725	0.108450	0.341370
0.60	0.075744	0.220314	0.256513
0.80	0.125950	0.270783	0.167702
1.00	0.182800	0.205316	0.077777
1.20	0.242804	0.302137	-0.008536
1.40	0.302010	0.202567	-0.085352
1.50	0.350083	0.260047	-0.146765
1.60	0.400547	0.235206	-0.188105
1.80	0.452660	0.105270	-0.207553
2.00	0.5077545	0.153030	-0.205844
2.20	0.514257	0.114123	-0.186066
2.40	0.533531	0.070628	-0.156761
2.60	0.540553	0.051767	-0.121631
2.80	0.554700	0.038030	-0.087200
3.00	0.550302	0.016577	-0.057440
3.20	0.551004	0.007517	-0.034335
3.40	0.552330	0.002381	-0.018120
3.60	0.552821	-0.000132	-0.007802
4.00	0.552621	-0.001070	-0.002101
4.20	0.552443	-0.001212	0.000488
4.40	0.552218	-0.001003	0.001300
4.60	0.552047	-0.000711	0.001430
4.80	0.551931	-0.000453	0.001124
5.00	0.551800	-0.000265	0.000766
5.20	0.551621	-0.000143	0.000472
5.40	0.551400	-0.000070	0.000268
5.60	0.551200	-0.000030	0.000142
5.80	0.551000	-0.000000	0.000070
6.00	0.551786	0.000000	0.000033
	0.551785	0.000000	

TABLE 6
TABLE OF UNIVERSAL FUNCTION F102

ETA	F	F'	F''
0.20	0.200000	0.200000	0.230000
0.22	0.204345	0.242174	0.101560
0.24	0.210351	0.276565	0.152160
0.26	0.216432	0.302072	0.111782
0.28	0.225000	0.321276	0.071276
0.30	0.222414	0.331503	0.032245
0.32	0.2100132	0.334000	-0.003255
0.34	0.135730	0.330664	-0.033156
0.36	0.101045	0.316400	-0.055840
0.38	0.104145	0.308870	-0.070556
0.40	0.204452	0.303040	-0.077474
0.42	0.221680	0.272340	-0.077660
0.44	0.235821	0.263231	-0.072752
0.46	0.247053	0.249463	-0.064537
0.48	0.255722	0.237531	-0.054654
0.50	0.262211	0.227628	-0.044422
0.52	0.266014	0.219727	-0.034752
0.54	0.270224	0.213652	-0.026220
0.56	0.272480	0.203148	-0.019273
0.58	0.273000	0.205020	-0.013372
0.60	0.274010	0.203711	-0.009028
0.62	0.275523	0.202240	-0.005863
0.64	0.275050	0.201302	-0.003658
0.66	0.276040	0.200728	-0.002101
0.68	0.276157	0.200300	-0.001250
0.70	0.276215	0.200200	-0.000603
0.72	0.276243	0.200007	-0.000366
0.74	0.276257	0.200044	-0.000185
0.76	0.276253	0.200012	-0.000089
0.78	0.276265	0.200005	-0.000041
0.80	0.276266	0.200000	-0.000018

TABLE 7

TABLE OF UNIVERSAL FUNCTION G111

ETA	F	F'	F''
2.00	0.000000	0.000000	-0.842084
2.20	-0.017082	-0.185071	-1.000478
2.40	-0.075820	-0.306034	-1.112838
2.60	-0.177015	-0.625032	-1.170002
2.80	-0.326627	-0.861376	-1.175695
3.00	-0.522101	-1.002555	-1.127748
3.20	-0.702060	-1.300064	-1.020017
3.40	-1.044205	-1.501621	-0.880771
3.60	-1.361222	-1.562022	-0.718357
3.80	-1.700000	-1.787720	-0.528002
4.00	-2.073737	-1.874112	-0.335501
4.20	-2.454014	-1.922470	-0.150330
4.40	-2.840364	-1.935452	0.017001
4.60	-3.226116	-1.917260	0.160732
4.80	-3.505526	-1.872000	0.278853
5.00	-3.773003	-1.807404	0.372413
5.20	-4.327300	-1.725410	0.444452
5.40	-4.563107	-1.630837	0.408006
5.60	-4.870000	-1.526700	0.530746
5.80	-5.273444	-1.415650	0.570448
6.00	-5.545003	-1.200157	0.503785
6.20	-5.702034	-1.178546	0.611828
6.40	-6.016200	-1.054720	0.526064
6.60	-6.214555	-0.920355	0.537541
6.80	-6.307412	-0.790200	0.646097
7.00	-6.534400	-0.660710	0.654053
7.20	-6.655100	-0.530047	0.661784
7.40	-6.740533	-0.405108	0.667754
7.60	-6.817166	-0.271045	0.673056
7.80	-6.857006	-0.135077	0.677828
8.00	-6.873407	0.000000	0.682167

TABLE 2
TABLE OF UNIVERSAL FUNCTION G112

ETA	F	F'	F''
0.20	0.000000	0.000000	-0.204085
0.30	-0.005136	-0.050182	-0.340464
0.40	-0.024084	-0.136500	-0.445693
0.50	-0.000081	-0.230048	-0.400307
0.60	-0.116712	-0.320121	-0.483386
0.70	-0.191014	-0.421100	-0.420485
0.80	-0.204164	-0.408344	-0.337884
0.90	-0.300845	-0.554592	-0.221880
1.00	-0.504371	-0.526500	-0.097026
1.10	-0.522802	-0.503258	0.021351
1.20	-0.742848	-0.570277	0.120710
1.30	-0.653360	-0.547427	0.103265
1.40	-0.250040	-0.503003	0.236046
1.50	-1.054504	-0.454622	0.253413
1.60	-1.140421	-0.404083	0.240447
1.70	-1.210351	-0.355006	0.231005
1.80	-1.283020	-0.311781	0.207026
1.90	-1.341400	-0.272767	0.182580
2.00	-1.302463	-0.230543	0.150400
2.10	-1.437142	-0.208701	0.130080
2.20	-1.470211	-0.182400	0.124674
2.30	-1.510204	-0.152712	0.113002
2.40	-1.530031	-0.137048	0.104207
2.50	-1.505200	-0.116021	0.097500
2.60	-1.580070	-0.097070	0.092255
2.70	-1.604461	-0.079024	0.087076
2.80	-1.618725	-0.062775	0.084353
2.90	-1.620610	-0.046242	0.081100
3.00	-1.637262	-0.030306	0.078364
3.10	-1.641775	-0.014008	0.075803
3.20	-1.643257	0.000000	0.073457

TABLE C
TABLE OF UNIVERSAL FUNCTION A113

ETA	F	F'	F''
0.00	1.000000	0.000000	-0.028315
0.20	-0.000304	-0.000137	-0.061125
0.40	-0.004012	-0.023633	-0.081607
0.60	-0.012443	-0.040022	-0.080086
0.80	-0.020304	-0.058400	-0.083886
1.00	-0.033663	-0.073740	-0.068028
1.20	-0.047027	-0.085110	-0.044622
1.40	-0.057366	-0.091302	-0.017704
1.60	-0.065010	-0.092256	0.008524
1.80	-0.073063	-0.098221	0.031028
2.00	-0.080047	-0.099282	0.047282
2.20	-0.085880	-0.099705	0.056407
2.40	-0.090000	-0.1050140	0.050105
2.60	-0.1050145	-0.1046520	0.056422
2.80	-0.1073550	-0.1035221	0.050175
3.00	-0.1173572	-0.1026583	0.042066
3.20	-0.1172105	-0.1010032	0.033500
3.40	-0.1181207	-0.1013153	0.025466
3.60	-0.1183407	-0.1008770	0.018535
3.80	-0.1184001	-0.1005653	0.012041
4.00	-0.1185704	-0.1003514	0.008675
4.20	-0.1186346	-0.1002100	0.005587
4.40	-0.1186671	-0.1001216	0.003456
4.60	-0.1186856	-0.1000676	0.002053
4.80	-0.1186956	-0.1000351	0.001171
5.00	-0.1187000	-0.1000184	0.000641
5.20	-0.1187036	-0.1000080	0.000337
5.40	-0.1187048	-0.1000040	0.000160
5.60	-0.1187054	-0.1000016	0.000081
5.80	-0.1187056	-0.1000005	0.000037
6.00	-0.1187056	0.0000000	0.000016

TABLE 12
TABLE OF UNIVERSAL FUNCTION F111

ETA	F	F'	F''
0.10	0.000000	0.000000	0.504208
0.20	0.000315	0.000270	0.387004
0.30	0.004124	0.154704	0.264755
0.40	0.009400	0.194512	0.131048
0.50	0.018110	0.227088	-0.006391
0.60	0.030402	0.192275	-0.130833
0.70	0.045350	0.152510	-0.253182
0.80	0.062200	0.093502	-0.320064
0.90	0.082243	0.023020	-0.357270
1.00	0.210777	-0.045600	-0.330500
1.10	0.204452	-0.105028	-0.256501
1.20	0.178008	-0.146162	-0.151070
1.30	0.147470	-0.165264	-0.039847
1.40	0.114310	-0.103083	0.057674
1.50	0.083353	-0.144243	0.125060
1.60	0.057273	-0.115504	0.156660
1.70	0.037340	-0.093700	0.155188
1.80	0.023500	-0.054567	0.133448
1.90	0.015120	-0.031140	0.100083
2.00	0.010607	-0.014605	0.065008
2.10	0.008002	-0.004306	0.037507
2.20	0.005850	0.000038	0.017171
2.30	0.003022	0.003010	0.004743
2.40	0.000850	0.003240	-0.001530
2.50	0.010200	0.002662	-0.003703
2.60	0.010723	0.001877	-0.003888
2.70	0.011025	0.001173	-0.003000
2.80	0.011205	0.000653	-0.002125
2.90	0.011200	0.000313	-0.001317
3.00	0.011330	0.000111	-0.000740
3.10	0.011340	0.000000	-0.000305

TABLE 11
TABLE OF UNIVERSAL FUNCTION F112

ETA	F	F'	F''
0.00	0.000000	0.000000	-0.059654
0.20	-0.310261	-0.102042	-0.260298
0.40	-0.077271	-0.307237	-0.071702
0.60	-0.174086	-0.500386	-0.055780
0.80	-0.300021	-0.767373	-0.007780
1.00	-0.400107	-0.940361	-0.813761
1.20	-0.503547	-1.080010	-0.663388
1.40	-0.613314	-1.201685	-0.454418
1.60	-1.101003	-1.257306	-0.106330
1.80	-1.416606	-1.278336	0.088546
2.00	-1.600601	-1.232287	0.367004
2.20	-1.690616	-1.133801	0.506588
2.40	-2.110412	-0.904466	0.774407
2.60	-2.302134	-0.830060	0.855125
2.80	-2.450050	-0.650402	0.848760
3.00	-2.566000	-0.405507	0.771035
3.20	-2.650540	-0.353224	0.647174
3.40	-2.700106	-0.230010	0.504576
3.60	-2.747654	-0.151103	0.366426
3.80	-2.771305	-0.090176	0.248064
4.00	-2.775120	-0.050211	0.156302
4.20	-2.772510	-0.025052	0.091514
4.40	-2.770175	-0.012102	0.040365
4.60	-2.777700	-0.004070	0.024227
4.80	-2.770417	-0.001653	0.010530
5.00	-2.770501	-0.000305	0.003795
5.20	-2.770600	0.000113	0.000088
5.40	-2.770500	0.000174	-0.000135
5.60	-2.770537	0.000117	-0.000356
5.80	-2.770521	0.000040	-0.000302
6.00	-2.770517	0.000000	-0.000104

TABLE 12
TABLE OF UNIVERSAL FUNCTION F113

ETA	F	F'	F''
0.00	0.000000	0.000000	-0.183868
0.20	-0.003675	-0.036745	-0.183460
0.40	-0.114000	-1.173106	-0.180288
0.60	-0.032872	-0.108306	-0.170283
0.80	-0.057937	-0.140551	-0.149217
1.00	-0.088720	-0.167000	-0.113847
1.20	-0.124103	-0.185048	-0.063382
1.40	-0.161077	-0.191500	-0.000640
1.60	-0.199856	-0.184005	0.067727
1.80	-0.235032	-0.164751	0.132352
2.00	-0.264072	-0.132003	0.183408
2.20	-0.297043	-0.092832	0.213200
2.40	-0.331062	-0.040242	0.218641
2.60	-0.367430	-0.006053	0.201000
2.80	-0.395014	0.022044	0.165038
3.00	-0.225007	0.058733	0.121170
3.20	-0.292142	0.078261	0.074508
3.40	-0.265204	0.088804	0.032144
3.60	-0.267134	0.001650	-0.002070
3.80	-0.220026	0.088600	-0.026694
4.00	-0.211050	0.081580	-0.042157
4.20	-0.195540	0.072251	-0.050027
4.40	-0.183110	0.061042	-0.052307
4.60	-0.171772	0.051573	-0.050030
4.80	-0.162456	0.041710	-0.047482
5.00	-0.155035	0.032544	-0.043108
5.20	-0.140337	0.024401	-0.038544
5.40	-0.145102	0.017213	-0.034208
5.60	-0.142307	0.010772	-0.030203
5.80	-0.140024	0.005065	-0.026850
6.00	-0.140327	0.000000	-0.023891

TABLE 13
TABLE OF UNIVERSAL FUNCTION F114

ETA	F	F'	F''
0.00	0.000000	0.000000	-0.243134
0.20	-0.205236	-0.254238	-0.200405
0.40	-0.222440	-0.110713	-0.354837
0.60	-0.053825	-0.105686	-0.403032
0.80	-0.101266	-0.277763	-0.434147
1.00	-0.165073	-0.367416	-0.437083
1.20	-0.240233	-0.452027	-0.402504
1.40	-0.346040	-0.525601	-0.326667
1.60	-0.450007	-0.580000	-0.213035
1.80	-0.570374	-0.600026	-0.073675
2.00	-0.690000	-0.500012	0.073271
2.20	-0.810074	-0.500551	0.207682
2.40	-0.920275	-0.527061	0.312317
2.60	-1.020123	-0.458377	0.376660
2.80	-1.112055	-0.380210	0.308530
3.00	-1.180176	-0.301527	0.383228
3.20	-1.233007	-0.228793	0.340055
3.40	-1.272370	-0.166214	0.283611
3.60	-1.300300	-0.115681	0.222050
3.80	-1.310453	-0.077160	0.164416
4.00	-1.330403	-0.040360	0.115504
4.20	-1.330700	-0.030282	0.077178
4.40	-1.344406	-0.017018	0.040141
4.60	-1.347210	-0.010052	0.020350
4.80	-1.348726	-0.005431	0.017333
5.00	-1.360524	-0.002803	0.009620
5.20	-1.340027	-0.001373	0.005108
5.40	-1.350110	-0.000628	0.002596
5.60	-1.350203	-0.000257	0.001262
5.80	-1.350234	-0.000080	0.000587
6.00	-1.350241	0.000000	0.000260

TABLE 14

TABLE OF UNIVERSAL FUNCTION F115

ETA	F	F'	F''
0.00	0.000000	0.000000	-0.023440
0.20	-0.000403	-0.005032	-0.027167
0.40	-0.002073	-0.010042	-0.030525
0.60	-0.004060	-0.017205	-0.032811
0.80	-0.008071	-0.023833	-0.033134
1.00	-0.014300	-0.030264	-0.030600
1.20	-0.021024	-0.035000	-0.025052
1.40	-0.028640	-0.040070	-0.016427
1.60	-0.036024	-0.042310	-0.005725
1.80	-0.045426	-0.042325	0.005586
2.00	-0.055300	-0.040152	0.015841
2.20	-0.061365	-0.035157	0.023616
2.40	-0.069080	-0.030031	0.028082
2.60	-0.073702	-0.025157	0.020146
2.80	-0.078150	-0.010460	0.027355
3.00	-0.081520	-0.014348	0.023630
3.20	-0.083055	-0.010070	0.010000
3.40	-0.085623	-0.006751	0.014323
3.60	-0.086715	-0.004315	0.010160
3.80	-0.087300	-0.002634	0.006808
4.00	-0.087800	-0.001535	0.004320
4.20	-0.088041	-0.000855	0.002600
4.40	-0.088160	-0.000454	0.001487
4.60	-0.088235	-0.000231	0.000800
4.80	-0.088268	-0.000112	0.000410
5.00	-0.088284	-0.000051	0.000206
5.20	-0.088291	-0.000022	0.000007
5.40	-0.088294	-0.000000	0.000043
5.60	-0.088295	-0.000003	0.000010
5.80	-0.088295	-0.000000	0.000007
6.00	-0.088295	0.000000	0.000002

TABLE 15

TABLE OF UNIVERSAL FUNCTION F119

ETA	F	F'	F''
0.00	0.300000	0.300000	-0.056419
0.20	-0.002772	-0.007447	-0.018049
0.40	-0.002467	-0.007220	0.020136
0.60	-0.003252	0.002510	0.056364
0.80	-0.001705	0.015258	0.080755
1.00	0.003230	0.035030	0.115647
1.20	0.012061	0.060013	0.131105
1.40	0.027897	0.087527	0.133602
1.60	0.047911	0.113316	0.121033
1.80	0.072704	0.135300	0.096867
2.00	0.101559	0.151300	0.061727
2.20	0.132001	0.150724	0.021524
2.40	0.164007	0.160014	-0.018012
2.60	0.195312	0.152000	-0.051711
2.80	0.225500	0.130001	-0.076028
3.00	0.252044	0.123224	-0.080583
3.20	0.274050	0.104812	-0.093051
3.40	0.293000	0.086545	-0.088575
3.60	0.305760	0.060735	-0.078049
3.80	0.322023	0.055135	-0.066804
4.00	0.331705	0.043002	-0.054566
4.20	0.330302	0.033230	-0.043366
4.40	0.345220	0.025530	-0.033082
4.60	0.347700	0.019517	-0.026564
4.80	0.353122	0.014705	-0.020034
5.00	0.355002	0.011040	-0.016765
5.20	0.357500	0.008017	-0.013707
5.40	0.350034	0.005513	-0.011452
5.60	0.350020	0.003400	-0.009750
5.80	0.350314	0.001504	-0.008457
6.00	0.350400	0.000000	-0.007425

TABLE 16

TABLE OF UNIVERSAL FUNCTION F117

ETA	F	F'	F''
0.00	0.000000	0.000000	-0.102003
0.20	-0.021012	-0.018470	-0.002750
0.40	-0.027133	-0.033070	-0.063175
0.60	-0.014000	-0.043731	-0.043326
0.80	-0.024352	-0.050428	-0.023740
1.00	-0.034707	-0.053307	-0.005316
1.20	-0.045452	-0.052710	0.010841
1.40	-0.055000	-0.049100	0.023662
1.60	-0.064000	-0.043526	0.032360
1.80	-0.073110	-0.035552	0.036582
2.00	-0.070570	-0.022134	0.036000
2.20	-0.064604	-0.022013	0.033870
2.40	-0.058441	-0.015732	0.028600
2.60	-0.051054	-0.010500	0.022500
2.80	-0.042753	-0.006693	0.016548
3.00	-0.033000	-0.003028	0.011275
3.20	-0.024307	-0.002100	0.007116
3.40	-0.024600	-0.001002	0.004123
3.60	-0.024031	-0.000300	0.002152
3.80	-0.024075	-0.000088	0.000971
4.00	-0.024077	0.000034	0.000335
4.20	-0.024067	0.000052	0.00038
4.40	-0.024054	0.000052	-0.000070
4.60	-0.024043	0.000045	-0.000089
4.80	-0.024036	0.000020	-0.000073
5.00	-0.024031	0.000017	-0.000050
5.20	-0.024028	0.000000	-0.000030
5.40	-0.024027	0.000004	-0.000017
5.60	-0.024025	0.000001	-0.000008
5.80	-0.024026	0.000000	-0.000004
6.00	-0.024026	0.000000	-0.000001

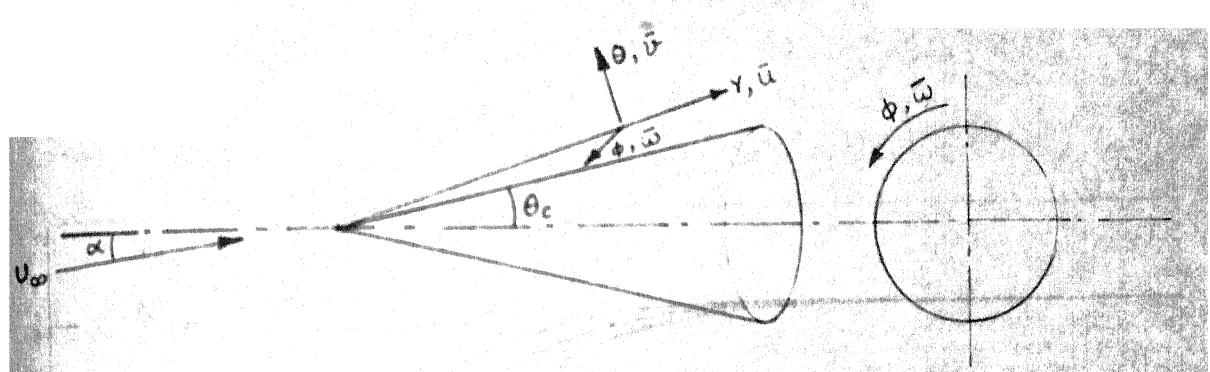


FIG 1 - COORDINATE SYSTEM FOR CONE

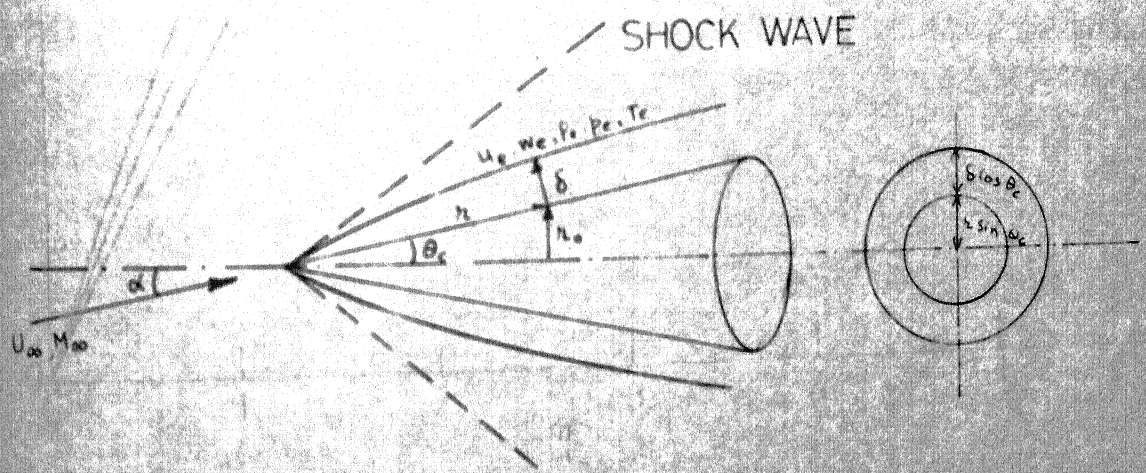


FIG 2 - NOTATIONS FOR CONE AT ANGLE OF ATTACK

θ_c = 5°, α = 0
M_∞ = 8.4925

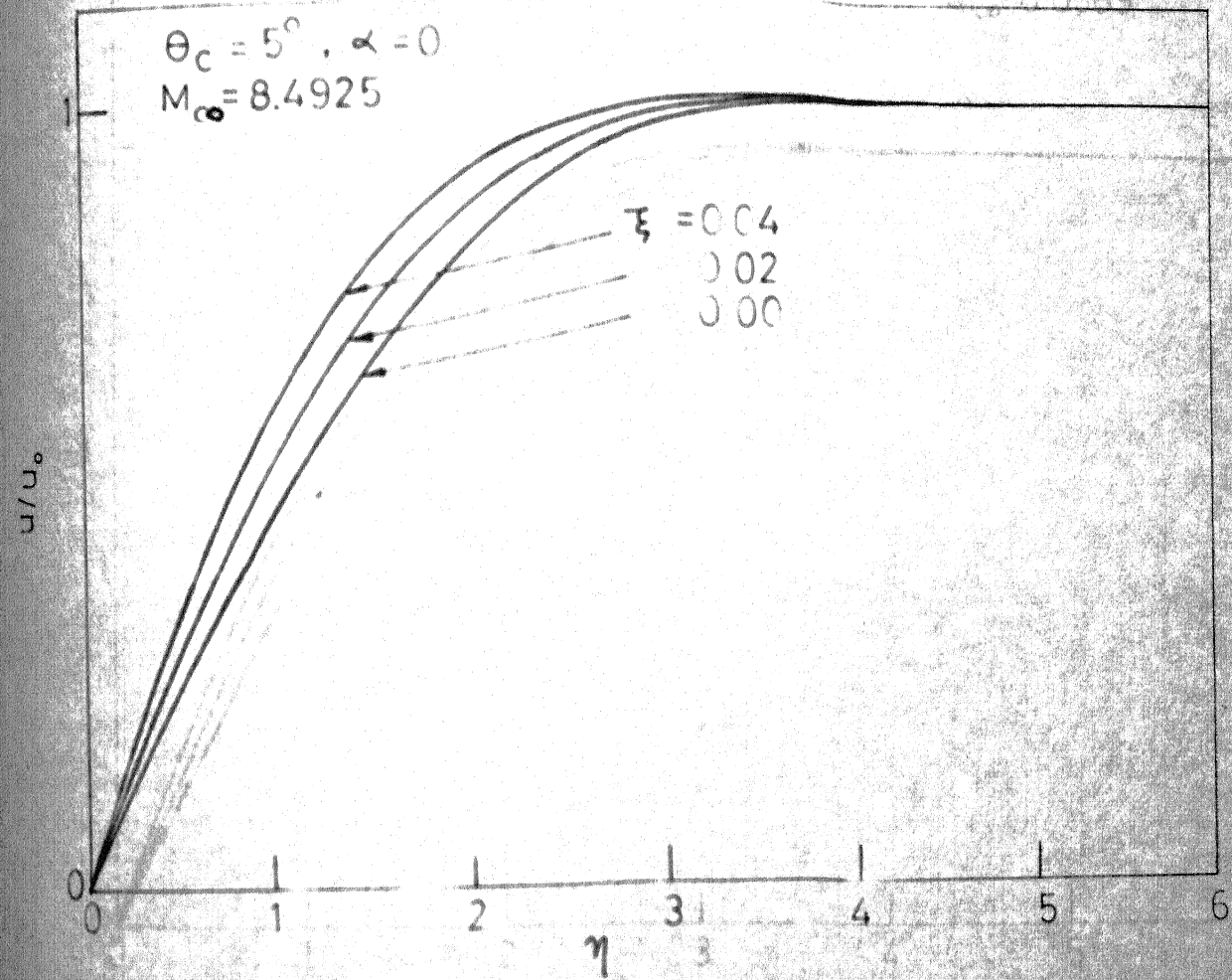


FIG. 3. VELOCITY PROFILE AT ZERO ANGLE OF ATTACK.

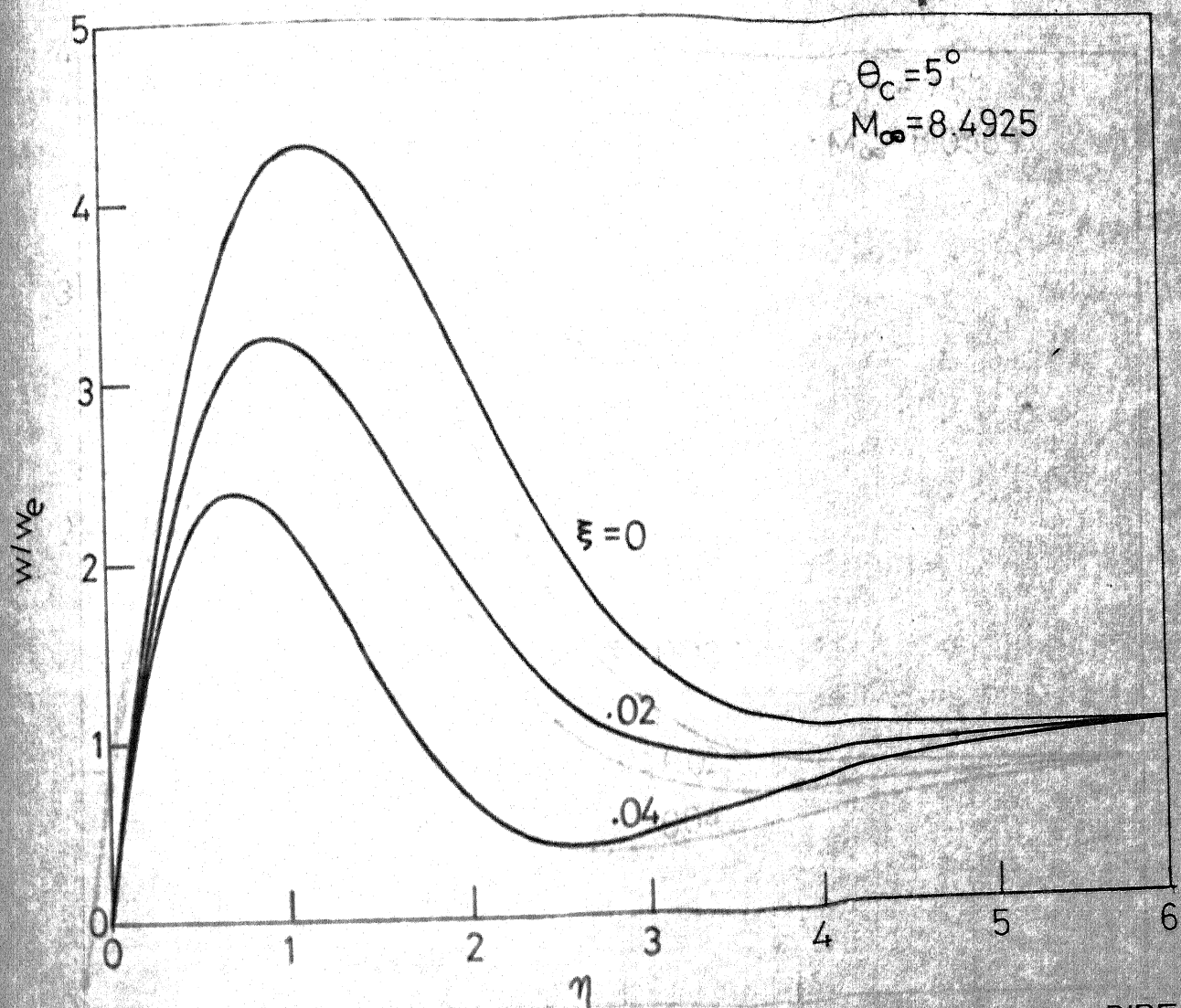


FIG. 5. VELOCITY PROFILE IN CIRCUMFERENTIAL DIREC

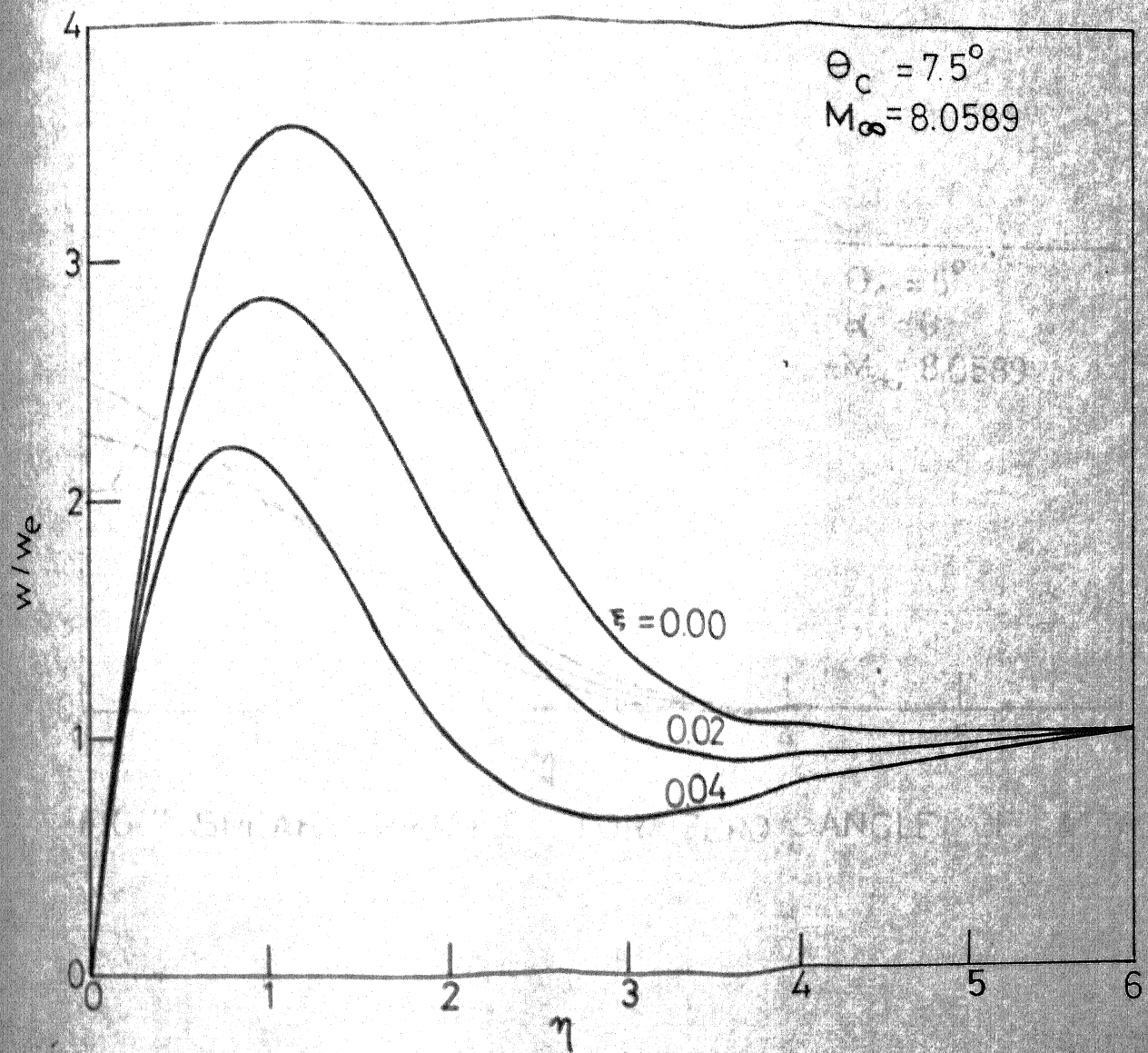


FIG.6-VELOCITY PROFILE IN CIRCUMFERENTIAL DIRECTION

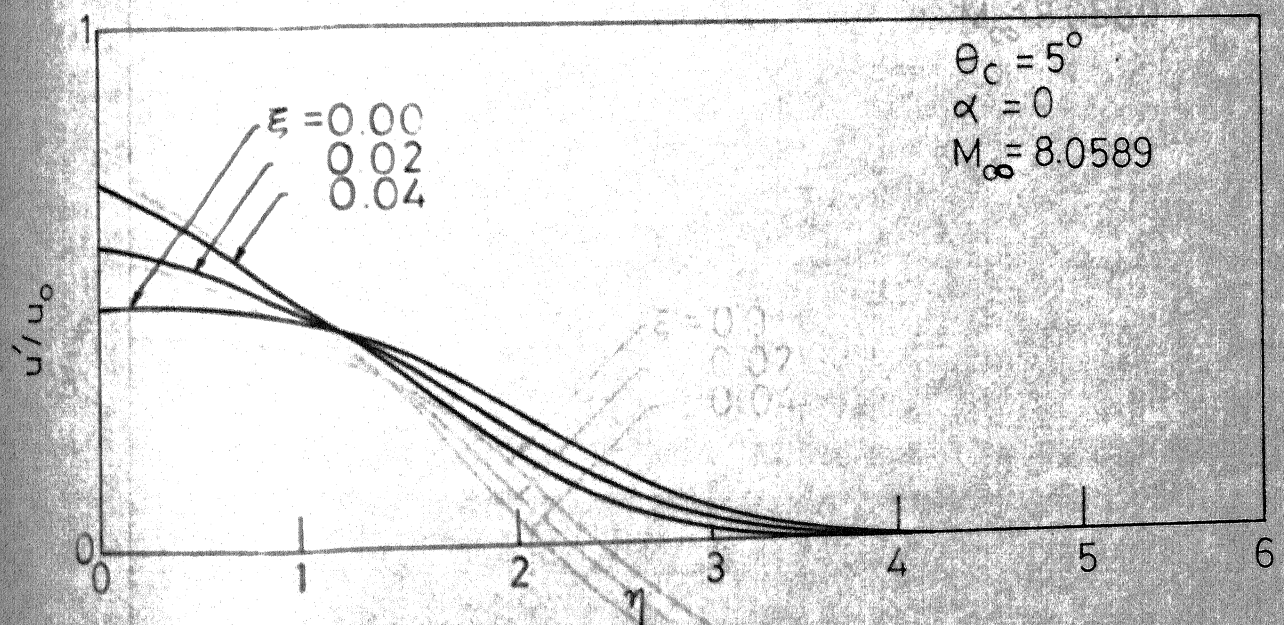


FIG. 7 - SHEAR PROFILE FOR ZERO ANGLE OF ATTACK

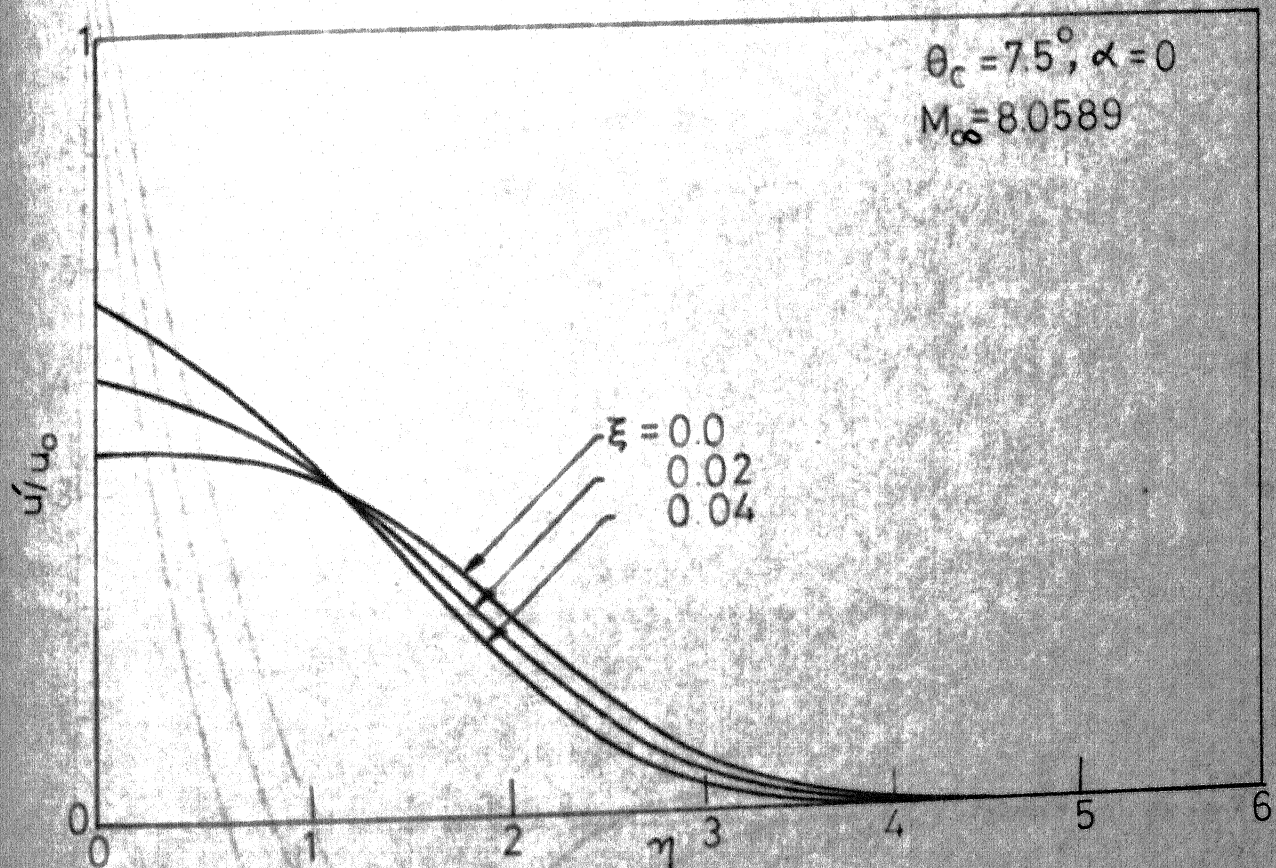


FIG. 8 - SHEAR PROFILE FOR ZERO INCIDENCE

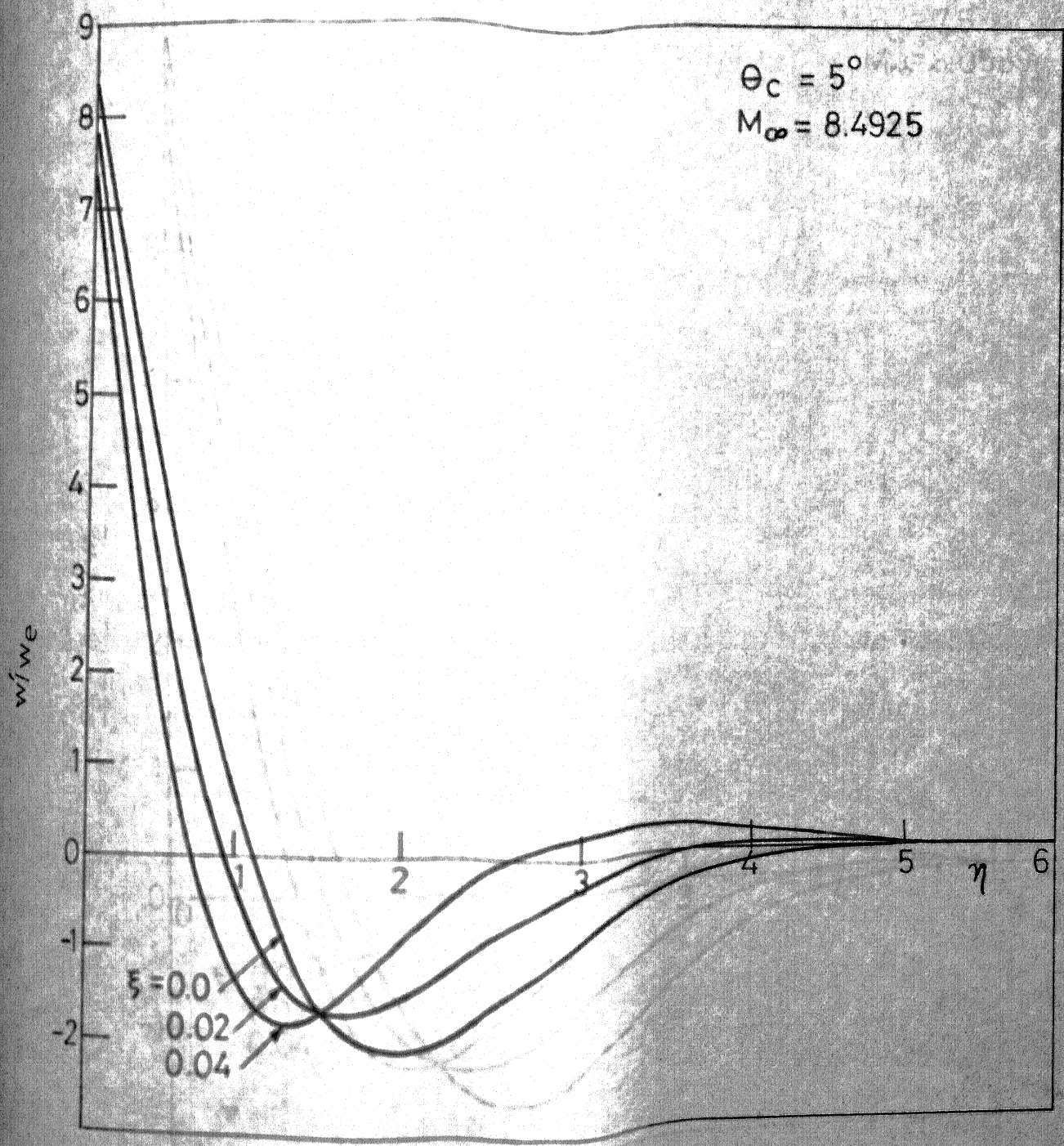


FIG.9 - CIRCUMFERENTIAL SHEAR PROFILE

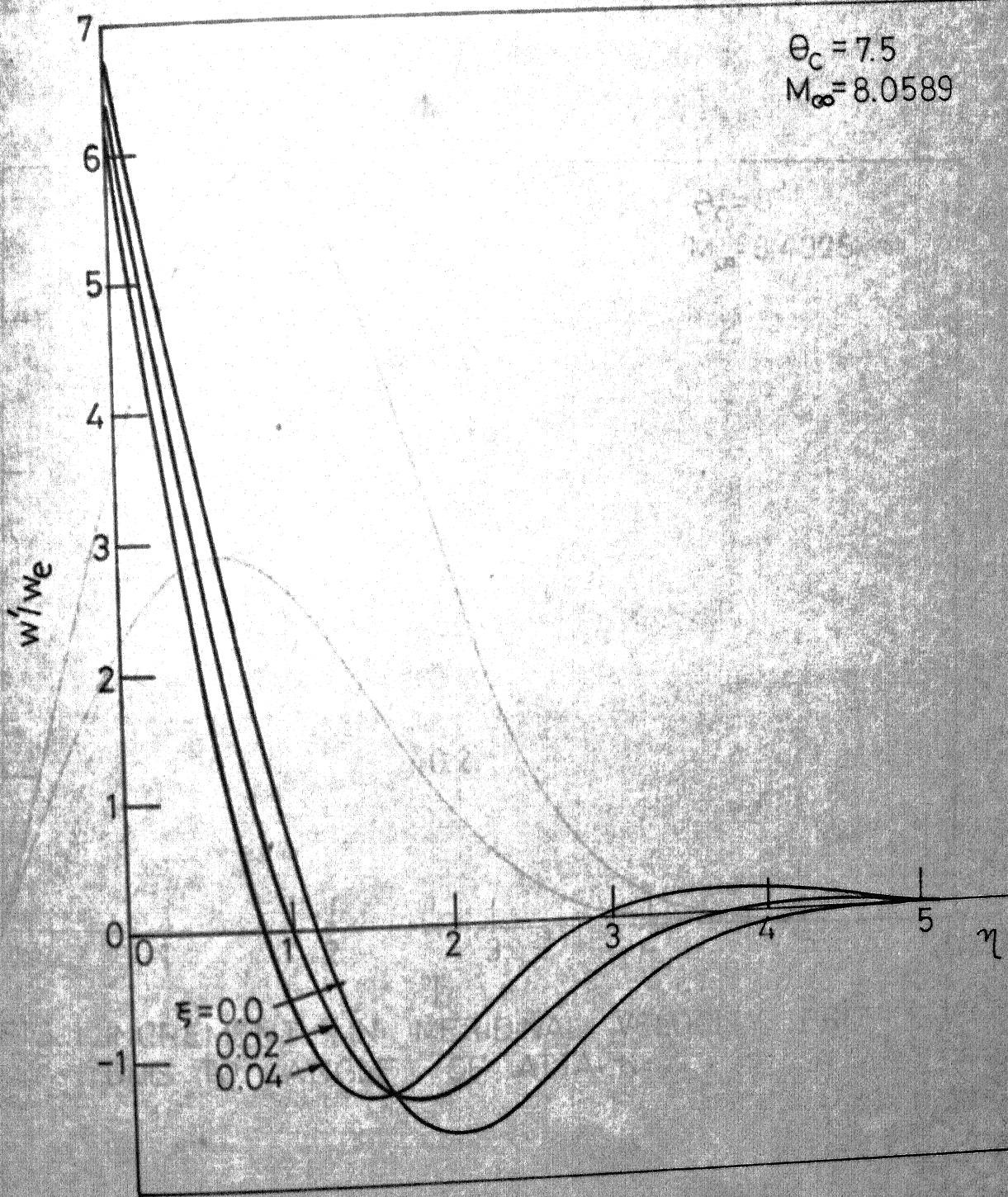


FIG.-10_CIRCUMFERENTIAL SHEAR PROFILE

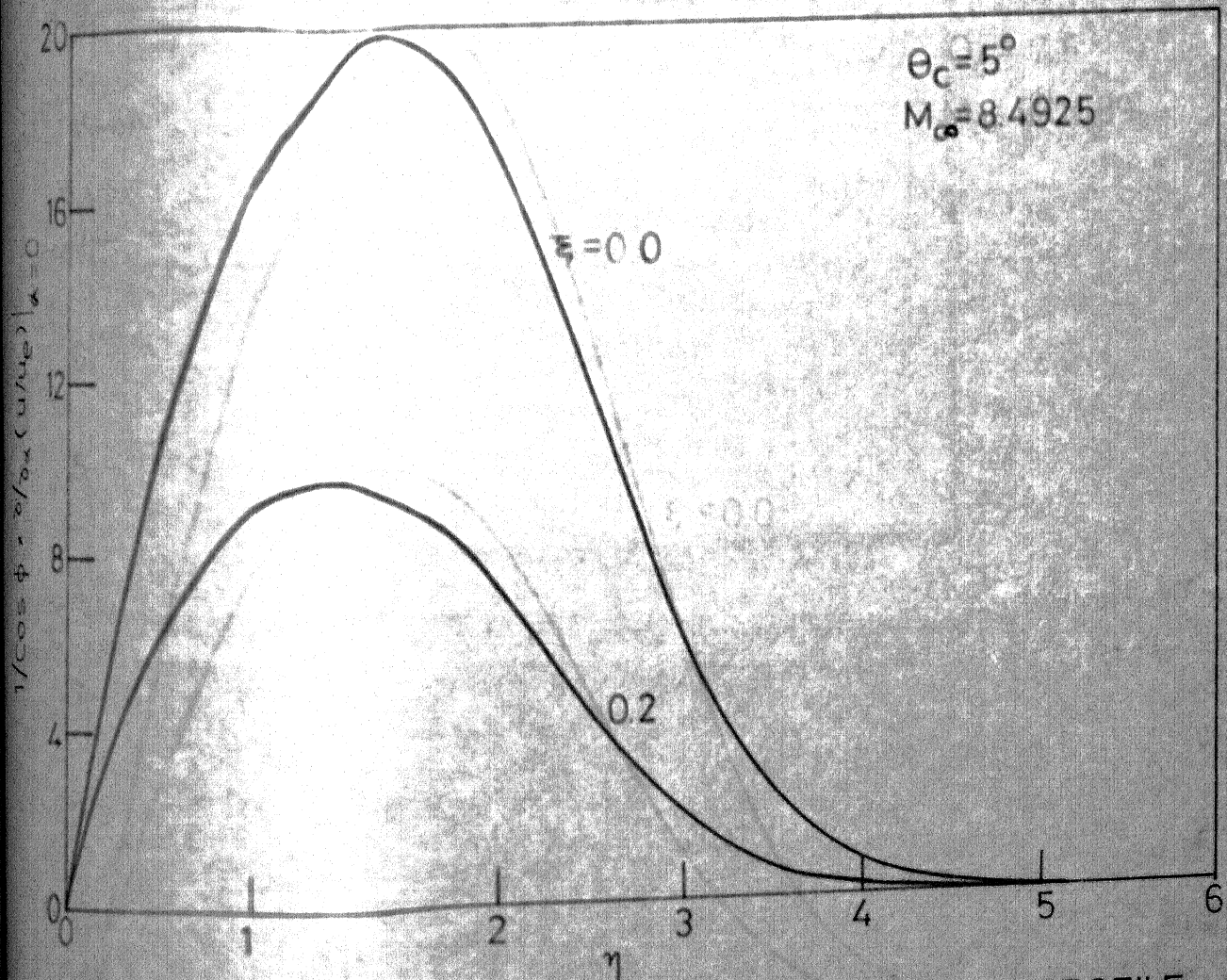


FIG.11. INCREMENT IN MERIDINAL VELOCITY PROFILE
DUE TO ANGLE OF ATTACK

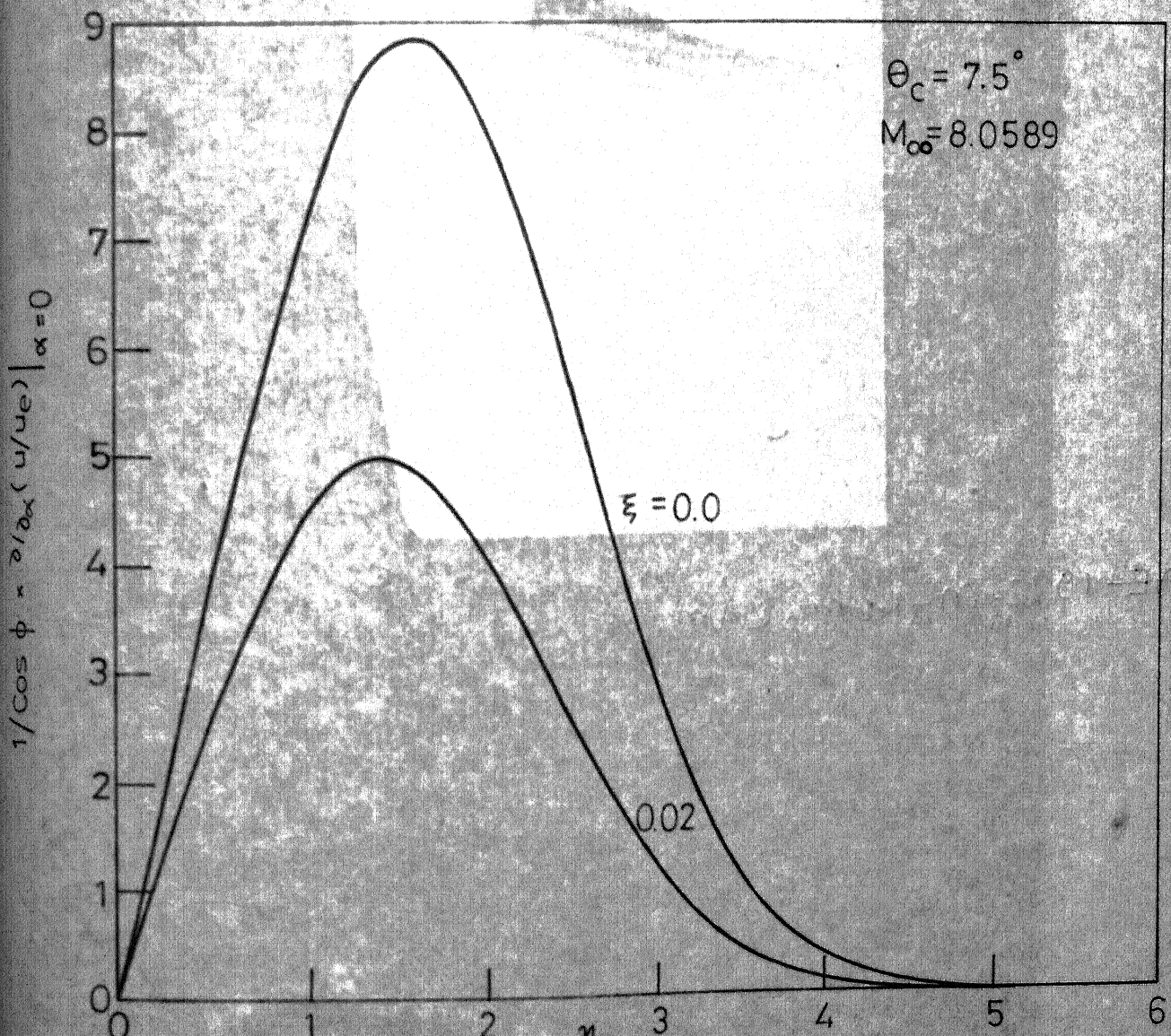


FIG.12 - INCREMENT IN MERIDINAL VELOCITY PROFILE
DUE TO ANGLE OF ATTACK .